www.elsevier.com/locate/developmentalbiology

Functional dissection of the Pax6 paired domain: Roles in neural tube patterning and peripheral nervous system development

Rosa-Eva Huettl, Simone Eckstein, Tessa Stahl, Stefania Petricca, Jovica Ninkovic, Magdalena Götz, Andrea B. Huber

PII: S0012-1606(15)30051-8
DOI: http://dx.doi.org/10.1016/j.ydbio.2015.07.009
Reference: YDBIO6823

To appear in: *Developmental Biology*

Received date: 4 February 2015
Revised date: 21 June 2015
Accepted date: 11 July 2015

Cite this article as: Rosa-Eva Huettl, Simone Eckstein, Tessa Stahl, Stefania Petricca, Jovica Ninkovic, Magdalena Götz and Andrea B. Huber, Functional dissection of the Pax6 paired domain: Roles in neural tube patterning and peripheral nervous system development, *Developmental Biology* http://dx.doi.org/10.1016/j.ydbio.2015.07.009

Functional dissection of the Pax6 Paired Domain: Roles in neural tube patterning and peripheral nervous system development

Rosa-Eva Huettl[1], Simone Eckstein[1], Tessa Stahl[2], Stefania Petricca[2], Jovica Ninkovic[2], Magdalena Götz[2], and Andrea B. Huber[1]

[1]Institute of Developmental Genetics, Helmholtz Zentrum München – German Research Center for Environmental Health (GmbH), Ingolstädter Landstraße 1, 85764 Neuherberg, Germany
[2]Institute of Stem Cell Research, Helmholtz Zentrum München – German Research Center for Environmental Health (GmbH), Ingolstädter Landstraße 1, 85764 Neuherberg, Germany

Corresponding author: Andrea B. Huber, email: andrea.huber@helmholtz-muenchen.de, phone: +49 89 3187 4117, fax; +49 89 3187 3099

Funding: This work was funded in part by the Deutsche Forschungsgemeinschaft DFG (SFB 870, Gö640/10.1 and Gö640/11-1). The funders had no role in study design, data collection and analysis, decision to publish, or preparation of the manuscript.

Abbreviations: bMN – branchiomotor neurons; Leca – Lens corneal adhesion; LMC – lateral motor column; MMC – medial motor column; Nkx2.2 – Nk2 homeobox 2; Pax6 – paired box 6; sMN – somatic motor neurons; Sp8 - trans-acting transcription factor 8; vMN – visceromotor neurons

Conflict of interest: The authors declare no conflict of interest.

Abstract

During development of the CNS, stem and progenitor cell proliferation, cell fate designation, and patterning decisions are tightly regulated by interdependent networks of key transcriptional regulators. In a genetic approach we analyzed divergent functionality of the PAI and RED sub-domains of the Pax6 Paired domain (PD) during progenitor zone formation, motor and interneuron development, and peripheral connectivity at distinct levels within the neural tube: within the hindbrain, mutation of the PAI sub-domain severely affected patterning of the p3 and pMN domains and establishment of the corresponding motor neurons. Exit point designation of hypoglossal axons was disturbed in embryos harboring either mutations in the PD sub-domains or containing a functional Pax6 Null allele. At brachial spinal levels, we propose a selective involvement of the PAI sub-domain during patterning of ventral p2 and pMN domains, critically disturbing generation of specific motor neuron subtypes and increasing V2 interneuron numbers. Our findings present a novel aspect of how Pax6 not only utilizes its modular structure to perform distinct functions via its paired and homeodomain. Individual sub-domains can exert distinct functions, generating a new level of complexity for transcriptional regulation by one single transcription factor not only in dorso-ventral, but also rostro-caudal neural tube patterning.

Key words: Pax6, bi-partite paired domain, neural tube patterning, somatic motor neurons, LMC, MMC, V2 interneurons

Introduction

Hindbrain and spinal cord harbour a complex circuitry of interneurons and motor neurons that are responsible for the regulation of locomotor activity. These neurons arise from distinct progenitor domains whose establishment critically depends on the complex cross-regulatory network of class I and class II transcription factors (reviewed in Jessell, 2000 and Alaynick et al., 2011). In the vertebrate neural tube, genetically distinct classes of motor neurons are generated from two different progenitor domains:

branchiomotor neurons (bMN) and visceromotor neurons (vMN) are exclusively generated at cranial levels and derive from progenitors in the p3 domain which lies adjacent to the floorplate and is characterized by the expression of the transcription factor Nkx2.2 (Briscoe et al., 1999; Guthrie, 2007; Pattyn et al., 2003; Sander et al., 2000). Somatic motor neurons (sMN) that will innervate target muscles of the tongue or the eye, and all sMN that are generated more caudally in the spinal cord derive exclusively from progenitor cells in the pMN domain in response to the expression of the transcription factors *Pax6*, *Olig2*, *Nkx6.1* and *Nkx6.2*. Excitatory and inhibitory V2, V1 and V0 interneurons are generated from the respective progenitor cells in the p2, p1 and p0 domains that are localized dorsally to the pMN and p3 domains. Furthermore, at spinal levels, V3 interneurons arise from the p3 domain in response to the bHLH transcription factor Sim1 (Briscoe et al., 2000; Ericson et al., 1997a; Goulding, 2009; Goulding and Pfaff, 2005).

The highly conserved class I transcription factor Pax6 was initially found to be a master regulator of eye development (Hill et al., 1991; reviewed in Gehring, 1996; Hever et al., 2006). Belonging to the family of paired box genes which all feature a characteristic 384 base pair DNA sequence that encodes the paired domain (PD), Pax6 also contains a paired-type homeodomain (HD) and a transactivation domain (TA). PD and HD recognize distinct DNA targets sites and regulate different molecular mechanisms, either in cooperation or separately. While both domains are involved in eye formation, loss and gain of function approaches have shown an involvement of the HD in the regulation of mature dopaminergic neuron survival, while only being of minor importance for developmental patterning mechanisms of the brain and spinal cord (Haubst et al., 2004; Ninkovic et al., 2010). Previous investigations in embryos harboring a truncated form of Pax6 which lacks the HD and TA and acts as a functional Null allele (*Pax6*^{Sey}) not only revealed impaired patterning, proliferation and neurogenesis within the brain (Bishop et al., 2002; Götz et al., 1998), but also characterized its importance for correct progenitor domain formation and boundary establishment at cranial and high cervical levels: Upon loss of cross-repressive effects with Nkx2.2, the p3 domain is enlarged on the expense of Olig2^{+} progenitor cells in the pMN domain. The increased expression of Nkx2.2 in *Pax6*^{Sey} mutant embryos triggers formation of bMN and vMN at

cranial levels, and of V3 interneurons at high cervical levels, while e.g. sMN that form the hypoglossal and the abducens nerves, as well as interneurons that are generated from the p2, p1 and p0 domains are lost (Ericson et al., 1997b; Osumi et al., 1997).

Interestingly, the PD itself is structured in a bipartite modular manner and contains an amino-terminal PAI and a carboxy-terminal RED sub-domain that each consists of a helix-turn-helix motif (Fig. 1A, Epstein et al., 1994). Recently, two mouse lines with selective point mutations in the PAI (*Pax6*^{Leca4}) or the RED (*Pax6*^{Leca2}) sub-domain of the Pax6 PD have been identified in an ENU-induced screen (Thaung et al., 2002). Selective mutation of each sub-domain revealed distinct roles of the PAI and the RED domain for neurogenesis and proliferation during forebrain development: Mutation of the RED domain increased proliferation of both apical and basal progenitors in the cerebral cortex, while ablation of the PAI domain had the opposite effect and decreased proliferation. Neurogenesis, however, was only affected in the *Pax6*^{Leca4} mutant mice, which displayed a smaller, shorter cerebral cortex and a thinner cortical plate with reduced neuron numbers that resembled the phenotype observed in Pax6 mutant mice with the functional Null allele (Walcher et al., 2013).

While the importance of Pax6 in controlling progenitor domain formation and neuronal fate at hindbrain levels has been well established, up to now Pax6-related control of progenitor cell identity and neuronal fate at spinal cord levels is only poorly understood. Interestingly, it appears that at more caudal levels, Pax6 becomes constantly less important for cross-repressive effects with Nkx2.2, while the zinc finger transcription factor Sp8 that to some extent is controlled by Pax6 acquires a more important role (Li et al., 2014). Intriguingly, the PAI and RED PD sub-domains manifest different functions during development of the cerebral cortex, while nothing is known about differential aspects of the PD sub-domains during cranial and spinal motor and interneuron development. In a genetic approach we analysed motor and interneuron formation at cranial levels in *Pax6*^{Leca2} and *Pax6*^{Leca4} mutant embryos and found that specifically the PAI, but not the RED domain is important for correct boundary formation between the p3 and pMN domains. Upon mutation of the PAI domain, a phenotype that is very reminiscent of what was observed in *Pax6*^{Sey} mutant embryos was observed for motor neuron generation: the p3 domain was enlarged on the expense of the pMN

domain, causing the formation of bMN and vMN, while sMN were reduced in number and motor projections of the abducens and hypoglossal nerves were absent or largely reduced. Intriguingly, neither mutation of the PAI or RED PD sub-domains affected generation of ventral interneuron subtypes, implicating a redundant function of both sub-domains for faithful generation of p2 and p1 progenitor zones.

At spinal brachial levels, investigation of progenitor zone formation revealed a similar phenotype in *Pax6*^{Sey} mutants as at cranial levels, and we observed a specific loss of motor neurons that constitute the medial motor column (MMC) and the lateral aspect of the lateral motor column (LMCl). Investigation of wholemount embryo preparations further corroborates these findings by revealing thinned motor projections of intercostal nerves and motor innervation of the dorsal forelimb. In contrast to this, in both *Pax6*^{Leca2} and *Pax6*^{Leca4} mutant embryos, boundary formation between the p3 and pMN domains occurred normally, probably also regulated through cross-repressive effects of Sp8 and Nkx2.2 at this important border. Intriguingly, however, we also observed a drop in sMN progenitors in *Pax6*^{Leca4} mutant embryos that is accompanied by a decrease of motor neuron numbers of the MMC and LMCl, and thinned projections of the respective nervous trajectories. In contrast to *Pax6*^{Sey} and *Pax6*^{Leca2} mutant embryos, the domain containing Sp8^{+} progenitors was enlarged dorsally upon mutation of the PAI domain, and we observed a selective expanse of the p2 domain, favouring specifically the generation of V2a and V2b interneurons.

Our results therefore underscore a differential functionality of the PAI and RED PD sub-domains during progenitor domain formation, as well as motor and interneuron generation. Furthermore, our data imply that specifically at brachial levels the PAI PD sub-domain is involved in correct establishment of the pMN and p2 progenitor zones by containment of V2 interneuron generation.

Materials and Methods

Mouse embryo preparation

The genotype of mouse embryos was determined as described for *Pax6*^{Leca2}, *Pax6*^{Leca4}, *Pax6*^{Sey}, and *Hb9::eGFP* (Hill et al., 1991; Thaung et al., 2002; Walcher et al., 2013; Wichterle et al., 2002). The day of vaginal plug was considered E0.5. Animals were

handled and housed according to the German Federal guidelines for the use and care of laboratory animals, and the study was approved by the Helmholtz Zentrum München Institutional Animal Care and Use Committee and the Regierung von Oberbayern.

Immunohistochemistry and cell quantification

The protocols for immunohistochemistry and wholemount antibody staining have been described previously (Huber et al., 2005; Huettl and Huber, 2011; Huettl et al., 2011). The following primary antibodies were used for fluorescent immunohistochemistry on cryosections or wholemount embryos: goat anti-Chx10 (1:250, Santa Cruz Biotechnology sc-21690), goat anti-FoxP1 (1:250, R&D Systems AF4534), goat anti-Gata2 (1:25, sc-9008), goat anti-Phox2a (1:100, sc-13229), goat anti-Sox1 (1:100, sc-1731), goat anti-Sp8 (1:200, sc-104661), mouse anti-En1 4G11, mouse anti-Isl1/2 39.4D5, mouse anti-Lim3 4E12, mouse anti-Neurofilament 2H3, mouse anti-Nkx2.2 74.5A5 (1:50, obtained from the Developmental Studies Hybridoma Bank developed under the auspices of the NICHD and maintained by The University of Iowa, Department of Biological Sciences, Iowa City, IA 52242), mouse anti-Ascl1 (1:100, BD Pharmigen 556604), rabbit anti-GFP (1:2000, Invitrogen A11122), rabbit anti-Olig2 (1:500, Chemicon AB9610), and rabbit anti-Sim1 (1:1000, Aviva ARP33296_P050). Antibody staining was visualized using fluorochrome-conjugated secondary antibodies (1:250; Molecular Probes; Jackson Dianova). Cells were quantified per hemisphere and section of the hindbrain or brachial spinal cord. Significance was calculated using the Mann-Whitney test.

In situ hybridization

In situ hybridization was performed as described before (Huber et al., 2005; Huettl et al., 2011) using mouse digoxigenin-labelled probes for *En1* (a kind gift from Nilima Prakash), and *Foxn4* (a generous gift from Mengqing Xiang, (Del Barrio et al., 2007).

Quantification of abducens and hypoglossal rootlet number and hypoglossal nerve thickness

The number of axons contributing to the abducens nerve was quantified by counting the projections leaving the neural tube (Fig. S1A). Hypoglossal rootlets were defined according to Fig. S1B. Thickness of the hypoglossal nerve was measured at the point where all projections contributing to the hypoglossal nerve converge to one nerve (CP in Fig. 1H, H'). Both sides of the embryos were analyzed. Significance was calculated using the Mann-Whitney test.

Quantification of pre-plexus fasciculation

Quantification of defasciculation of motor and sensory fibers before the plexus region in E10.5 whole mount embryos has been described before (Huettl et al., 2011). Briefly, the individual thickness of the 6 spinal nerves contributing to the forelimb-plexus was measured ("a" in Fig. 3A), summarized, and normalized to the length of the spinal cord from which these 6 projections originate ("b" in Fig. 3A) to determine a fasciculation coefficient. Both sides of the embryos were analyzed. Significance was calculated using the Mann-Whitney test.

Quantification of distal advancement

To quantify the distance of ingrowth of motor axons into the forelimb of E12.5 embryos, the length of the distal-most motor fiber ("x" in Fig. 3F) was measured starting from the reference point (RP) and normalized with the length of the forelimb ("y" in Fig. 3F). Both forelimbs were analyzed. Significance was calculated using the Mann-Whitney test.

Quantification of Sp8 and Ngn1 coefficient

The size of the domains containing either $Sp8^+$ or $Ngn1^+$ cells was measured ("a" in Fig. 6A, H) and divided by the size of the entire spinal cord ("b" in Fig. 6A, H). Both hemispheres were analyzed. Significance was calculated using the Mann-Whitney test.

Results

Mutation of the Pax6 PAI PD sub-domain and the functional Null allele of Pax6 impair formation of somatic motor projections at cranial levels

Previous analyses by Ericson et al., revealed severe defects in the formation of the somatic motor hypoglossal projection upon mutation of Pax6 due to a fate change of sMN to bMN/vMN following changed progenitor cell generation (Ericson et al., 1997b). To determine the role of the PAI and RED sub-domains in sMN generation at cranial levels, we investigated the formation of abducens and hypoglossal projections in wholemount embryo preparations by Hb9::eGFP fluorescence in somatic motor projections (Wichterle et al., 2002). In control embryos, first somatic motor axons leave the hindbrain at E10.5 and have formed a fasciculated abducens projection that targets the lateral rectus muscle of the eye by E11.5 (Fig. 1C, C'). At the level of the hypoglossal nerve, somatic motor rootlets have left the neural tube, fasciculated at the convergence point (CP in Fig. 1H, H') and a distinct projection has joined the first cervical nerves at the vagal plexus. From here, hypoglossal projections start to turn towards the tongue by E10.5 and have passed the vagal plexus 1 day later (Fig. 1 H, H'). In *Pax6*^{Sey} mutant embryos, only very few, if any projections were seen at the level of the abducens nerve, and we never observed formation of a distinct projection targeting the eye at any analyzed time point (arrows in Fig. 1F, F', G). At the level of the hypoglossal nucleus, only very few hypoglossal rootlets (arrow in Fig. 1K) were observed and also the first cervical projection (C1) was severely reduced in size in all analyzed *Pax6*^{Sey} mutant embryos when compared to control littermates at E10.5. This phenotype is maintained at E11.5, where very few, if any hypoglossal (arrow in Fig 1K') and high cervical projections (C1) leave the neural tube and no hypoglossal nerve itself was found (Fig. 1K' – M). We furthermore observed aberrantly projecting GFP-positive somatic motor axons projecting along the spinal accessory nerve (SAN, arrowhead in Fig. 1K') in *Pax6*^{Sey} mutant embryos.

Investigation of embryos where the RED sub-domain of the Pax6 PD was mutated showed that at E10.5 abducens axons exit the neural tube in normal numbers and have formed a fasciculated projection towards the eye that is indistinguishable from the control situation by E11.5 (Fig. 1D, D', G). Accordingly, the hypoglossal nerve is assembled by an unchanged number of hypoglossal rootlets and starts turning towards the tongue by E10.5 in *Pax6*^{Leca2} mutant embryos (Fig. 1I, L, M). Intriguingly, however, while the hypoglossal projection itself appears normal also one day later at E11.5 (Fig.

1I', L, M), we also observed aberrantly projecting somatic motor fibers in the SAN (arrowhead in Fig. 1I').

In contrast, analyses of *Pax6*^{Leca4} mutant embryos revealed that abducens projections are absent in 2/3 of the analyzed animals and severely diminished in the rest (0.33 ± 0.33) when compared to control littermates (6.42 ± 0.68) at E10.5 (Fig. 1E, G). Also at E11.5, hardly any abducens fibers were detected in *Pax6*^{Leca4} mutant embryos (1.38 ± 0.46 vs. 8.25 ± 0.45; Fig. 1E', G). At the level of the hypoglossal nucleus, reduced numbers of hypoglossal rootlets leave the brainstem from the caudal-most positions of the hypoglossal nucleus (10.40 ± 1.11 vs. 18.92 ± 0.97) and form a thinner projection that, however, turns correctly for the tongue at E10.5 (7.79 ± 2.70 vs. 25.34 ± 0.95) in embryos where the PAI sub-domain was mutated (arrow in Fig. 1J, L, M). At E11.5, the phenotype of *Pax*^{Leca4} mutant embryos is more heterogeneous when compared to what we observed in *Pax6*^{Sey} mutants, where the hypoglossal projection itself was missing entirely and only a few fibers leaving the brainstem were observed (Fig. 1K). Here, we found embryos in which the hypoglossal nerve formed a projection towards the tongue, or, as depicted in Fig. 1 J', hypoglossal rootlets met, but only a very thin, short projection migrated towards the vagal plexus. However, in all analyzed embryos, hypoglossal rootlets were significantly reduced in number (13.88 ± 1.53) when compared to control littermates (21.44 ± 1.30, Fig. 1L). At the CP, the hypoglossal projection was always significantly thinner (14.94 ± 2.66) than in littermate controls (26.18 ± 1.45, Fig. 1M). Interestingly, we found similar aberrant somatic motor projections in the SAN in *Pax6*^{Leca4} as already observed in *Pax6*^{Leca2} and *Pax6*^{Sey} mutant embryos (arrowhead in Fig. 1J'). Analysis of coronal sections of the hindbrain at the level of the hypoglossal nucleus that was localized by expression of Hb9::eGFP revealed that in all three *Pax6* mutant lines, somatic motor axons project to dorsal regions and aberrantly exit the neural tube at dorsal positions (Fig. S2A – D).

We therefore conclude that the function of the PAI sub-domain is necessary for the correct establishment of the somatic motor projections of the abducens and the hypoglossal nerves of the hindbrain. Furthermore, our data suggest an involvement of both PAI and RED sub-domains in exit point designation of somatic motor projections at cranial levels.

Mutation of the PAI PD sub-domain affects sMN, but not interneuron generation similar to *Pax6*^{Sey} at hindbrain levels

To assess whether PD sub-domain specific functions are required for generation of genetically distinct motor neuron progenitors at the levels of the abducens and the hypoglossal somatic motor nuclei, we detected progenitor cells in the p3 and pMN domains by immunohistochemistry against Nkx2.2 and Olig2, respectively, on coronal sections of embryos that express *Hb9::eGFP* in all sMN and thus allow for an easy detection of both somatic motor nuclei in the developing hindbrain. In embryos where the RED domain was mutated, we observed normal generation of p3 and pMN domain at the level of the abducens nucleus. Quantification of the expansion of the p3 domain and number of Nkx2.2^{+}, as well as quantification of Olig2^{+} somatic motor neuron progenitors showed no significant alterations in *Pax6*^{Leca2} mutant embryos when compared to control littermates at the time points E10.5 and E11.5 (Fig. 2A, A', C, C', G – I). Accordingly, progenitor domains were established normally at hypoglossal levels at both evaluated time points in embryos where the RED domain was mutated (Fig. 2B, B', D, D', G – I). Quite contrary, quantification of Nkx2.2^{+} cells revealed a significant increase of p3 progenitors at both abducens and hypoglossal levels in *Pax6*^{Leca4} mutant embryos. According to what was observed in embryos harboring the functional Null allele of Pax6 (Ericson et al., 1997b), the number of Olig2^{+} sMN progenitors was significantly reduced at both investigated time points at the levels of the abducens and the hypoglossal nuclei. The remaining sMN progenitors were interspersed in between elevated numbers of progenitors of the p3 domain that was expanded in size at the level of the abducens nerve and the hypoglossal nerve when compared to littermate controls (Fig. 2E, E', F, F', G – I).

To analyze whether the altered patterning of the p3 and pMN domains causes a fate change during cranial motor neuron establishment, we assessed generation of bMN, vMN and sMN at hindbrain levels. The paired homeodomain transcription factors Phox2a and Phox2b critically contribute to the generation of motor neurons that derive from the p3 domain (Brunet and Pattyn, 2002). Employing immunohistochemical staining against Phox2a we visualized bMN and vMN at the level of the abducens and the

hypoglossal nuclei in E10.5 embryos. To localize the position of the abducens and the hypoglossal levels we took advantage of Hb9::eGFP expression, which is expressed only in sMN and their projections (Fig. 1, Fig. S2, Fig. 3D – F). Additionally, we utilized GFP expression to quantify sMN. In control embryos, a subset of Phox2a^{+} cells was observed in ventral regions, were these neurons are born. A second pool of neurons has already migrated to more dorsal positions, from where the axons of these neuronal populations exit the neural tube and innervate muscles of the head and neck (Fig. 3A, A'). In embryos where the RED domain was mutated, Phox2a^{+} motor neurons were also found at dorsal and ventral positions in the neural tube. Numbers of bMN and vMN did not vary significantly in *Pax6^{Leca2}* mutant embryos when compared to littermate controls (Fig. 3C, C', G). sMN were generated at normal numbers at both abducens and hypoglossal levels (Fig. 3E, E', G), reflecting our observations in wholemount embryo preparations, where both somatic motor projections were established normally in *Pax6^{Leca2}* mutants. *Pax6^{Leca4}* mutant embryos showed a phenotype similar to that of *Pax6^{Sey}* mutants where the abducens nerve was missing entirely. Analysis of sMN at this level of the hindbrain revealed a severe reduction to 1.81 ± 0.34, while in control embryos 9.30 ± 0.64 GFP^{+} neurons were observed per section in the abducens nucleus (Fig. 3F, G). Accordingly, investigation of p3-derived motor neurons revealed a significant increase of Phox2a^{+} motor neurons at the level of the abducens nerve in *Pax6^{Leca4}* mutant embryos to 80.81 ± 13.50 when compared to control littermates (42.03 ± 3.80, Fig. 3E, G). At hypoglossal levels, the phenotype observed in *Pax6^{Leca4}* mutant embryos was more heterogeneous than in *Pax6^{Sey}* mutant embryos – however, the hypoglossal projection was reduced: indeed, analysis of sMN numbers showed a significant decrease of Hb9::eGFP^{+} motor neurons in the hypoglossal nucleus of *Pax6^{Leca4}* mutants (22.05 ± 3.05), thus forming a thinner projection, when compared to control embryos (32.95 ± 2.08). Corresponding to that, numbers of Phox2a^{+} bMN and vMN were significantly elevated at the level of the hypoglossal nucleus in embryos where the PAI domain was mutated (Fig. 3E', F', G).

Previous investigations concerning Pax6 function during embryonal development also found that in *Pax6^{Sey}* mutant embryos, V2 and V1 interneurons are lost within the hindbrain (Ericson et al., 1997b). We set out to explore the differential role of the Pax6

PD sub-domains in interneuron generation by immunohistochemical detection of $Chx10^+$ V2a interneurons and $En1^+$ V1 interneurons at E10.5 (Fig. 3B, B'). Intriguingly, we observed V2a and V1 interneurons in both *Pax6*^{Leca2} and *Pax6*^{Leca4} mutant embryos. Neurons were generated at normal numbers and were correctly positioned within the cranial neural tube at both abducens and hypoglossal levels (Fig. 3D – E', H).

Taken together, our findings suggest that a functional PAI domain is required for correct progenitor domain patterning by establishing cross-repressive effects between the p3 and the pMN domains. The subsequent generation of the respective motor neuron subtypes and their peripheral projections at cranial levels is affected according to altered patterning of the progenitor zones upon mutation of the PAI PD sub-domain, while the RED domain plays only a minor, if any role during progenitor zone and motor neuron establishment. Interestingly, interneuron generation was not impaired by mutation of any of the Pax6 PD sub-domains, suggesting that one functional Pax6 PD sub-domain is sufficient for faithful establishment of ventral interneuron populations.

Late, but not initial forelimb innervation is impaired in *Pax6*^{Sey} mutant embryos or upon mutation of the PAI PD sub-domain

While the importance of Pax6 for motor and interneuron generation at hindbrain levels is well established, its role at spinal levels is only poorly understood. We therefore analyzed innervation of the developing forelimb in wholemount embryo preparations at relevant time points: By E10.5, the 6 spinal nerves that contribute to the brachial plexus and will later on innervate the forelimb have converged in the plexus region at the base of the limb (Fig. 4A). At E11.5, first target specific bundles have formed and invaded the limb in control embryos (Fig. S3A). By E12.5, a stereotypical innervation pattern of the four main nerves innervating forelimb musculature is established: The musculocutaneous nerve (msc) will innervate proximal ventral limb musculature. Radial (1, 2) and ulnar nerves (4) innervate dorsal musculature of the proximal and distal forelimb and paw, respectively, while the median nerve (3) targets muscles of the distal ventral limb and paw (Fig. 4F).

At E10.5, a plexus was formed in embryos with a functional Null allele of Pax6, as well as in embryos where either the RED or the PAI sub-domains of the Pax6 PD were

mutated. To determine whether pre-plexus fasciculation was affected or whether spinal nerves were thinned due to loss of fibers we calculated a fasciculation coefficient and found no significant differences when comparing *Pax6*^{Leca2}, *Pax6*^{Leca4}, and *Pax6*^{Sey} mutant embryos to their respective control littermates (Fig. 4A – E). Accordingly, initial target specific branches were formed normally in all three *Pax6* mutant mouse lines at E11.5 (Fig. S3A – D, arrowheads). By E12.5, distinct nerve branches are formed in all mutant lines. Gross morphology and positioning of those projections is comparable to what we observed in control embryos. However, while in *Pax6*^{Leca2} mutant embryos quantification of distal advancement of Hb9::eGFP^{+} motor axons into the limb and analysis of the individual thickness of these motor projections innervating the forelimb did not show any differences (Fig. 4G, J, K), aberrations were observed in *Pax6*^{Sey} and in *Pax6*^{Leca4} mutants. In embryos where the PAI PD sub-domain was mutated, distal advancement of motor nerves was not affected. Quantification of the individual thickness of motor nerves innervating the forelimb showed that the median and ulnar nerves were established normally when compared to control littermates (Fig. 4H, K). Contrary to our observations in *Pax6*^{Leca2} mutants, musculocutaneous (msc in Fig. 4H, 13.47 ± 0.69 vs. 16.10 ± 0.76) and radial nerves (2, arrow in Fig. 4H, 17.05 ± 0.75 vs. 21.85 ± 1.42), as well as the first branch of the radial nerve (1, arrowhead in Fig. 4H, 4.98 ± 0.88 vs. 8.08 ± 0.68) were significantly thinner in *Pax6*^{Leca4} mutant embryos. In *Pax6*^{Sey} mutant embryos, distal advancement of motor axons into the distal limb was slightly reduced when compared to control littermates (0.60 ± 0.007 vs. 0.65 ± 0.006; Fig. 4I, J). Quantification of the individual thickness of motor nerves showed that median and ulnar projections are established normally in *Pax6*^{Sey} mutants (Fig. 4I, K). The musculocutaneous (msc in Fig 4I) and radial (arrow in Fig. 4I) nerves, however, were significantly thinner in all analyzed mutant embryos (msc: 12.18 ± 0.73; rad: 11 ± 0.66), a phenotype which is very reminiscent of what we observed in *Pax6*^{Leca4} mutant embryos. Furthermore, in 2/3 of the analyzed embryos, the first ramus branching off the radial nerve was missing entirely in *Pax6*^{Sey} mutant embryos, while in the remaining embryo it was severely reduced (arrowhead in Fig. 4I, 1.97 ± 0.72 vs. 8.08 ± 0.68).

These findings suggest a minor role of *Pax6* and both PD sub-domains during early targeting of motor axons to the plexus region and primary formation of target

specific branches. However, our observations argue for an involvement of Pax6 and especially the PAI domain during the sophisticated establishment of distinct motor branches at later stages.

Generation of LMCl motor neurons is impaired upon mutation of the Pax6 PAI PD sub-domain and in *Pax6^{Sey}* mutant embryos

The alterations in peripheral motor innervation of *Pax6^{Sey}* and *Pax6^{Leca4}* mutant embryos prompted us to investigate progenitor zone formation and establishment of limb-innervating motor neurons at brachial levels. As already observed at cranial levels, establishment of the p3 domain that contains Nkx2.2^{+} progenitor cells that at spinal levels give rise to V3 interneurons was not altered in *Pax6^{Leca2}* mutant embryos when compared to control littermates. Furthermore, also Olig2^{+} motor neurons progenitors were generated in normal numbers in embryos where the RED domain was mutated (Fig. 5B – C', F – H). In *Pax6^{Sey}* mutant embryos we observed an expansion of the p3 domain (E10.5: 80.08 µm ± 8.07 vs 38.12 µm ± 2.96; E11.5: 147.1 µm ± 13.37 vs. 55.61 µm ± 3.54). Numbers of p3 progenitor cells were increased (E10.5: 54.20 ± 4.46 vs. 30.88 ± 1.17; E11.5: 61.04 ± 3.50 vs. 40.52 ± 2.48) while numbers of Olig2^{+} pMN progenitors were markedly reduced (E10.5: 6.47 ± 2.76 vs. 22.01 ± 2.73; E11.5: 2.871 ± 1.12 vs. 14.06 ± 1.12) in *Pax6^{Sey}* mutant embryos (Fig. 5E – H), a phenotype that is reminiscent of previous analyses of cranial patterning and motor neuron generation (Ericson et al., 1997b). Interestingly, while at cranial levels *Pax6^{Leca4}* mutant embryos show a similar phenotype with an increased p3 domain on the expense of the pMN domain as *Pax6^{Sey}* mutants, at brachial levels the p3 domain is not expanded and also numbers of Nkx2.2^{+} progenitor cell do not differ significantly from control littermates (Fig. 5D, D', F, G). Furthermore, in contrast embryos with a functional Null allele of Pax6, in *Pax6^{Leca4}* mutant embryos normal numbers of Olig2^{+} motor neuron progenitors were observed at E10.5 (Fig. 5C, H). Intriguingly, however, by E11.5 we observed a drop in motor neuron progenitor numbers in *Pax6^{Leca4}* mutant embryos to 2.87 ± 1.12 while in control embryos at this time point 14.06 ± 1.12 Olig2^{+} progenitor cells were observed per spinal cord hemisphere at brachial levels (Fig. 5B', D', H). We therefore investigated the establishment of spinal motor neurons that form the lateral and medial aspects of the

LMC which later on innervate respective dorsal and ventral limb musculature, respectively. Immunohistochemistry against forkhead box P1 (FoxP1) labels all motor neurons of the LMC (Palmesino et al., 2010). For distinction of the medial and lateral LMC we used antibody staining against Isl1, determining LMCm motor neurons as $FoxP1^{+}/Isl1^{+}$ (magenta dashed lines in Fig. S4, Fig. 5), while LMCl motor neurons are characterized by FoxP1 expression in absence of Isl1 (cyan dashed lines in Fig. S4, Fig. 5). Motor neurons that will form the lateral aspect of the LMC leave the cell cycle after LMCm motor neurons and have to migrate past these neurons to their final positions in the lateral ventral spinal cord (Kania et al., 2000). By E10.5, in control embryos and also in all three *Pax6* mutant lines, motor neurons of both molecular subtypes are generated, however, sub-columns have not separated yet topographically, and the proportion of $FoxP1^{+}/Isl1^{+}$ LMCm motor neurons contributing to the entire LMC exceeds that of $FoxP1^{+}/Isl1^{-}$ motor neurons of the LMCl (Fig. S4A – E). By E11.5, in wildtype embryos motor neurons of the medial and lateral LMC constitute 50% of the entire LMC, respectively, and have separated into two specific sub-columns within the ventral horn at brachial levels (Fig. S4F, J). In embryos where either the RED or the PAI sub-domain of the Pax6 PD were mutated, we observed no alterations in initial segregation and proportioning of motor neurons of the LMC in the respective medial and lateral sub-columns (Fig. S4G, H, J). In $Pax6^{Sey}$ mutant embryos $FoxP1^{+}/Isl1^{+}$ and $FoxP1^{+}/Isl1^{-}$ motor neurons segregate into lateral and medial aspects of the LMC (Fig. 4I). However, upon quantification of neurons contributing to the respective sub-columns, we found that the proportions are not equally distributed as observed in control embryos, but that the proportions of the LMCm (0.56 ± 0.03) exceeds the proportion of the LMCl (0.44 ± 0.029, p≤ 0.03, Fig. S4J). At E12.5, we observed a reduction of individual nerve thickness of specific nerve branches that innervate dorsal limb musculature in whole mount preparations of both $Pax6^{Sey}$ and $Pax6^{Leca4}$ mutant embryos. When we quantified proportions of motor neurons contributing to the LMCm and LMCl, we found that in contrast to the wildtype situation where $FoxP1^{+}/Isl1^{+}$ and $FoxP1^{+}/Isl1^{-}$ motor neurons contribute to the entire LMC in equal proportions (Fig. 5I, M), in $Pax6^{Sey}$ and $Pax6^{Leca4}$ mutant embryos the LMCl subpopulation is markedly reduced when compared to the proportion of the LMCm (Fig. 5K – M, $Pax6^{Sey}$: 0.46 ± 0.02 vs 0.54 ± 0.02, p≤ 0.03;

Pax6^{Leca4}: 0.46 ± 0.01 vs. 0.54 ± 0.01, p≤ 0.0006). In *Pax6*^{Leca2} mutant embryos, no alterations in the individual thickness of motor nerves innervating the distal forelimb were observed at E12.5. We also observed no significant alterations (p=0.06) in LMC motor neuron segregation at this time point (Fig. 5J, M).

Thus, in the brachial spinal cord, the functional Null allele of *Pax6* impacts on progenitor domain formation in a similar way as at cranial levels with an expansion of the p3 domain at the expense of the pMN domain. Intriguingly, neither mutation of the RED or the PAI domain affects formation of the p3 domain, and also motor neuron progenitors are initially generated at normal numbers. Nevertheless, the overall reduction of motor neuron progenitors in *Pax6*^{Sey} mutant embryos, as well as the drop in progenitor cell numbers at E11.5 in *Pax6*^{Leca4} may account for reduced numbers of late-born LMCl motor neurons.

Sp8 facilitates boundary formation between p3 and pMN progenitor zones and establishment of medial motor column (MMC) neurons

Previous investigations showed that the zinc finger protein Sp8 plays a supplementary role to Pax6 during the establishment of the boundary between the p3 and the pMN domains. While at rostral levels of the neural tube, Pax6 alone is responsible for the establishment of this boundary, at brachial level loss of Pax6 function leads to a rather mosaic pattern of an expanded p3 domain and interspersed motor neuron progenitors (Fig. 5E; E'). At lumbar levels, *loss of Pax6* alone does not impair formation of boundaries between p3 and pMN domain at all. Upon combined abolishment of Pax6 and Sp8, however, disruption of the p3/pMN domain boundary was observed along the entire rostro-caudal axis of the spinal cord (Li et al., 2014).

Given the fact that Sp8 is also involved in the establishment of motor neurons upon repression of Nkx2.2 expression and is retained in a subpopulation of MMC neurons (Li et al., 2014), we analyzed the expression pattern and generation of MMC motor neurons in embryos with a functional Null allele of *Pax6*, or where the RED or PAI PD sub-domains of the Pax6 PD were mutated. In control embryos, expression of Sp8 overlaps with expression of Olig2 in motor neuron progenitors, while it forms a boundary with Nkx2.2^{+} progenitor cells of the p3 domain at E11.5 (Fig. 6A). Furthermore, Sp8^{+}

cells leave the progenitor domains of the ventricular zone and migrate to more ventro-lateral positions within the brachial spinal cord (arrows in Fig. 6A). Also in embryos, where the RED PD sub-domain was mutated, the domain containing $Sp8^+$ cells was established normally and formed a boundary with progenitors of the p3 domain. Moreover, $Sp8^+$ cells were migrating to the ventral horn of the spinal cord (arrows in Fig.6B, E, F). In *Pax6*^{Sey} mutant embryos we observed an overlap of the expanded domain containing $Nkx2.2^+$ and $Sp8^+$ cells (bracket in Fig. 6D). While the $Sp8^+$ domain was established more or less normally according to its dorso-ventral extent (Fig. 6E), we observed a marked decrease of neurons leaving the ventricular zone and migrating to the ventral horn (arrows in Fig. 6D, 3.81 ± 1.62 vs. 16.28 ± 1.61). Interestingly, in *Pax6*^{Leca4} mutant embryos, a clear border was formed between the p3 and the pMN domain by $Sp8^+$ cells, prohibiting dorsal expansion of the p3 domain, however, the domain containing $Sp8^+$ cells itself was expanded dorsally when compared to control littermates (362.90 ± 9.72 vs. 263.10 ± 13.99, $p \leq 0.01$). In accordance with the drop of $Olig2^+$ motor neuron progenitors, however, we observed that significantly less $Sp8^+$ cells migrated to lateral positions in the ventral horn of the spinal cord when compared to the wildtype situation (2.91 ± 1.39 vs. 15.63 ± 2.20). We next analyzed formation of the MMC utilizing fluorescent immunohistochemistry against Isl1 and Lim3. Upon mutation of the RED Pax6 PD sub-domain, no alterations in motor neurons numbers within the medial motor columns were detected when compared to control embryos (Fig. S5A, B, E). Also a closer investigation of $Isl1^+/Lim3^+/Sp8^+$ motor neurons revealed no significant difference in the generation of motor neurons that form this specific sub-population of the MMC (Fig. 6G, H, K) in *Pax6*^{Leca2} mutant embryos in comparison with wildtype embryos.

In contrast, mutation of the PAI Pax6 PD sub-domain, and also the functional Null allele of Pax6 resulted in a significant reduction of motor neurons that comprise the medial motor column (*Pax6*^{Leca4}: 10.97 ± 1.36, *Pax6*^{Sey}: 9.86 ± 1.90) when compared to control embryos (19.30 ± 1.23, Fig. S5A, C – E). A closer investigation of these motor neurons according to the expression of Sp8 revealed that indeed also the amount of these cells was significantly reduced in *Pax6*^{Leca4} (1.76 ± 0.60) and *Pax6*^{Sey} (1.15 ± 0.58) mutant embryos when compared to littermate controls (7.31 ± 0.32, Fig. 6G, I – K). To

further investigate the impact of this loss of MMC neurons, we analyzed the establishment of intercostal projections in wholemount embryo preparations by quantifying a fasciculation coefficient for the first 7 intercostal nerves. In *Pax6*^{Leca2}, intercostal projections were established normally and showed no alterations in the coefficient, when compared to littermate controls (Fig. S5G, K, N). Quite contrary, intercostal projections were reduced in thickness in both *Pax6*^{Leca4} and *Pax6*^{Sey} mutant embryos, resulting in a significantly reduced coefficient for both analyzed time points (Fig. S5H, I; L – N), reflecting the loss of MMC motor neurons within the spinal cord.

We therefore conclude that either a functional PAI or RED PD sub-domain is sufficient to establish correct boundaries between the p3 and the pMN domain. While Sp8 appears to contribute to this boundary formation, mutation of the PAI domain results in a marked reduction of Sp8^{+} MMC motor neurons and their peripheral projections. Furthermore, specifically the PAI domain appears to be involved in the developmental containment of Sp8^{+} progenitor cells at more dorsal positions of the spinal cord.

Expression of *Ngn1* and *2* is altered upon selective mutation of the PAI PD sub-domain

Proneural basic helix-loop-helix (bHLH) transcription factors play an important role in triggering neuronal differentiation. For instance, bHLH factors of the Neurogenin (Ngn) family, namely Ngn1 and Ngn2, promote cell cycle exit and coordinate neurogenesis from different neuronal progenitors, before they are downregulated upon differentiation of motor and interneuron subpopulation in the ventral spinal cord (Bertrand et al., 2002; Farah et al., 2000; Lee et al., 2005; Quinones et al., 2010; Scardigli et al., 2001). Our observations showed a decrease in sMN precursors in embryos where the Pax6 PAI PD sub-domain was mutated. Furthermore, while the boundary between Sp8^{+} pMN and Nkx2.2^{+} p3 progenitor domains was established normally, the Sp8^{+} domain was expanded towards more dorsal positions of the brachial spinal cord. These findings prompted us to investigate Ngn expression in domains containing neuronal precursors for motor and interneuron generation at brachial spinal levels. In *Pax6*^{Leca2} mutant embryos, *Ngn1* and *2* were normally expressed at dorsal and ventral positions within the spinal cord, when compared to control littermates (Fig. 6H, I,

L-N). The functional Null allele in *Pax6*^{Sey} mutant embryos resulted in a wildtype-like expression of *Ngn1* (Fig. 6K, L), while *Ngn2* expression was present, but largely reduced (Fig. 6P). Interestingly, in *Pax6*^{Leca4} mutant animals, the domain containing *Ngn1*$^{+}$ cells was enlarged according to the enlargement of the domain containing Sp8^{+} precursors (Fig. 6K, L; 0.42 ± 0.022) when compared to control littermates (0.28 ± 0.01, p≤ 0.004). Furthermore, also expression of *Ngn2* was upregulated along the ventricular zone, and, as opposing to what we observed upon selective mutation of the RED PD sub-domain or in embryos bearing a functional Null allele of Pax, *Ngn2* was still expressed in the pMN domain (arrow in Fig. 6O), and thus can promote cell cycle exit of Olig2^{+} progenitors. Given the fact that *Pax6*^{Leca4} mutant embryos show decreased motor neuron numbers, and both *Ngn1* and *2* have been shown to trigger generation of interneurons and/or motor neurons upon interaction e.g. with Olig2, this prompted us to further investigate interneuronal subtype generation in the ventral spinal cord.

V2a and V2b interneuron numbers are increased in number upon mutation of the Pax6 PAI PD sub-domain

The three different V2 interneuron subpopulations derive from a common p2 domain, which is located dorsally to the pMN domain (Fig. S6A). The Lim HD transcription factor Lim3 promotes differentiation of Delta-like-4^{+} progenitors to V2a interneurons that express the homeobox transcription factor Chx10 (Crone et al., 2008). We found comparable total numbers of Lim3^{+} cells in *Pax6*^{Leca2} and *Pax6*^{Sey} mutant embryos when compared to control littermates, however, in *Pax6*^{Sey} mutant embryos the dorso-ventral extent of these neurons that give rise to V2a interneurons was diminished (Fig. S6B, C, E – G, p<0.001). Interestingly, while in *Pax6*^{Leca4} mutant embryos Lim3^{+}/Isl1^{+} neurons that constitute the MMC where reduced in number (Fig. S5C, E), the total number of Lim3^{+} cells in the ventral spinal cord was elevated almost 2-fold to 120.9 ± 7.91 cells per spinal cord hemisphere when compared to 66.83 ± 8.56 cells in wildtype embryos (Fig. 7D, E, p<0.001). Furthermore, close to the ventricular zone these cells covered a larger dorso-ventral extent than in control embryos (110.1 µm ± 1.56 vs. 68.29 µm ± 1.99, Fig. S6B, D, F, G)

Progenitor cells in the p2 domain that express *Foxn4* and Ascl1 upon activation of Notch1 block molecular pathways that lead to the formation of V2a interneurons and are driven towards a V2b/c fate (Del Barrio et al., 2007; Yang et al., 2006). We performed *in situ* hybridization against *Foxn4* and fluorescent immunohistochemistry against Ascl1 to analyze their expression pattern in the p2 domain. When compared to control embryos, we could not detect a difference in the number or the extent of the domain containing *Foxn4*$^{+}$ progenitor cells in embryos where the RED PD sub-domain was mutated or in *Pax6*^{Sey} mutant embryos (Fig. S6H, I, K - M). Interestingly, while the extent of the domain containing Ascl1^{+} cells was not altered in *Pax6*^{Sey} mutant embryos, the number of Ascl1^{+} cells itself was diminished in *Pax6*^{Sey} mutant embryos (Fig. S6Q – S, $p \leq 0.01$). This was not the case upon selective mutation of the Pax6 RED PD sub-domain (Fig. S6O, R, S). Intriguingly, we observed a drastic increase of the size of the p2 domain containing *Foxn4*$^{+}$ and Ascl1^{+} cells, as well as an increased amount of these V2b interneuron progenitors upon mutation of the PAI PD sub-domain (Fig. S6 J, L, M, P, R, S).

Despite being generated in the same progenitor domain in the spinal cord, differentiated V2 interneurons acquire separate molecular identities and obtain different functions during adulthood. Excitatory Chx10^{+} V2a interneurons are found already by E10.5 in wildtype embryos (data not shown) and establish a distinct patterning with two well-defined neuronal pools in the brachial ventral spinal cord by E11.5 (Fig. 7A, B). Inhibitory Gata2^{+} V2b interneurons form similar pools in-between V2a interneurons, and V2b derived Sox1^{+} V2c interneurons gather in a medio-ventral position within the ventral spinal cord (Fig. 7A, G). *En1*$^{+}$ V1 interneurons and Sim1^{+} V3 interneurons that are generated from respective precursors in the p1 and p3 domains are located dorsally to V2 interneurons, or ventral to the zone where sMN are generated, respectively (Fig. S6A, Fig. 7A). At cranial and high cervical levels, V1 and V2 interneurons were observed to be absent, while V3 interneurons were increased due to a fate change from sMN to the V3 neuronal subtype in *Pax6*^{Sey} mutant embryos (Ericson et al., 1997b). Investigation of interneuron generation at brachial levels in *Pax6*^{Sey} mutant embryos revealed that according with the smaller progenitor domain, V2a interneurons are not absent, however, they are generated at lower numbers by E11.5 (20.58 ± 2.06, Fig. 7E,

F) when compared to control littermates (42.35 ± 3.74. Also V2b and V2c interneurons that derive from common progenitors were diminished in *Pax6*^{Sey} mutant embryos (Fig. 7J – L). In accordance with our data from cranial and high cervical levels, we found a complete absence of *En1*$^{+}$ V1 interneurons from *Pax6*^{Sey} mutant brachial spinal cord (Fig. 7P, Q), while *En1* expression e.g. in the lateral mesenchyme of the shoulder was not affected (Fig. S7). Furthermore, consistent with the expansion of the p3 domain, we also found enhanced generation of V3 interneurons in embryos with a functional Null allele (Fig. 7U, V). Previous investigations of *Pax6*^{Leca2} mutant embryos concerning progenitor zone formation revealed no obvious differences from the wildtype situation. In accordance, also analyses of spinal V1, V2, and V3 interneuron populations did not show significant alterations in interneuron cell numbers. V2a, V2b, and V2c interneurons were generated at normal numbers and were correctly localized within the brachial ventral spinal cord (Fig. 7, C, F, H, K, L). Also V1 and V3 interneurons were correctly positioned and showed no alterations in cell number in embryos where the Pax6 RED PD sub-domain was mutated (Fig. 7N, Q, S, V).

Intriguingly, upon mutation of the PAI PD sub-domain, we found that already at E10.5, V2a interneuron numbers are increased significantly (data not shown). This phenotype is evident even more drastically one day later, where Chx10^{+} V2a interneurons are rather spread over the entire medio-lateral extent between ventricular zone and the zone where sMN of the LMC and MMC reside. Cell numbers were increased more than twofold from 43.83 ± 4.12 cells per spinal cord hemisphere in wildtype embryos to 94.48 ± 5.81 cells in *Pax6*^{Leca4} mutant embryos (Fig. 7D, F). Interestingly, the increase of V2a is not due to a fate change of V2b interneurons due to an altered molecular setup of progenitor cells: In accordance with the increased numbers of V2b progenitors in the p2 domain, we also found an increase of Gata2^{+} V2b interneurons to 59.31 ± 12.43 cells in mutant embryos, when compared to 27.20 ± 1.74 cells in control littermates (Fig. 7I, K). Interestingly, the numbers of V2c interneurons that derive from a subset of V2b interneurons were not altered in number upon mutation of the Pax6 PAI PD sub-domain (Fig. 7I; L). Within the hindbrain we observed an expansion of the p3 domain at the expense of the pMN domain in *Pax6*^{Leca4} mutant embryos, leading to an increase of p3 derived motor neurons on the expense of sMN as

observed in *Pax6*^{Sey} mutant embryos. At brachial spinal level, this expense of the p3 domain and increased V3 interneuron generation was still observed in *Pax6*^{Sey} mutants, while in *Pax6*^{Leca4} mutant embryos the p3 domain was established normally in size and progenitor cell number. Consistent with these findings, the number of V3 interneurons was normal (Fig. 7T, V). Interestingly, while *Ngn1* has been reported to trigger V1 interneuron generation (Quinones et al., 2010), V1 interneurons that derive in the p1 progenitor zone dorsally of the altered p2 domain were established in normal numbers in *Pax6*^{Leca4} mutant embryos even though the domain containing *Ngn1*$^{+}$ precursors was enlarged (Fig. 6I) when compared to littermate controls (Fig. 7O, Q).

We therefore conclude that the Pax6 PAI PD sub-domain acquires distinctive roles in cranial and brachial spinal cord: At cranial levels it promotes generation of sMN, while loss of function favors generation of bMN and vMN. In contrast to cranial levels, where the PAI PD sub-domain does not play a role in interneuron generation, it is specifically involved in pMN-p2 boundary formation and the containment of V2a and V2b interneuron generation at brachial levels, while no effects were observed on the generation of V1 and V3 interneurons. Intriguingly, loss of function of the Pax6 RED PD sub-domain can be compensated for in most of the analyzed paradigms.

Discussion

Locomotor behavior depends on the precise formation of connections between motor neurons and their peripheral target muscles and requires the coordinated activity of numerous neuronal subtypes. Thus, developmental regulator genes occupy crucial positions in the genetic networks that tightly control faithful stem and progenitor cell proliferation, as well as cell fate, patterning decisions, and axonal connectivity. Within the vertebrate hindbrain, cross-repressive interaction between the Shh-induced transcription factor Nkx2.2 and the Shh-repressed transcription factor Pax6 characterizes the respective p3 and pMN progenitor domains that give rise to distinct motor neuron populations (Ericson et al., 1997b; Osumi et al., 1997). Interestingly, the bi-partite PD of Pax6 is which is mainly involved in neuronal generation reveals a differential functionality of the PAI and RED sub-domains during cortical development

(Walcher et al., 2013), raising the question whether also at hindbrain and spinal levels, neuronal generation may depend on sub-domain specific activity of Pax6 (summarized in table 1).

The Pax6 PAI PD sub-domain specifically facilitates patterning of ventral motor progenitor domains in the hindbrain

The pairs of class I and class II transcription factors that refine progenitor domain boundaries within the developing neural tube are potent repressors of each other's expression (Briscoe et al., 2000). Upon loss of this cross-repressive interaction e.g. in *Pax6*^{Sey} mutant embryos, the ventral p3 progenitor domain expands to more dorsal regions of the neural tube, on the expense of more dorsally localized progenitor domains and their respective derivatives (Ericson et al., 1997b; Osumi et al., 1997; Takahashi and Osumi, 2002). The intriguing fact that Pax6 not only utilizes its modular structure to perform distinct functions via its PA and HD (Haubst et al., 2004; Ninkovic et al., 2010), but even individual sub-domains of the PD that can exert distinct functions (Walcher et al., 2013) generates a new level of complexity for transcriptional regulation by one and the same transcription factor. Interestingly, only upon mutation of the Pax6 PAI PD sub-domain, p3-pMN domain patterning and subsequent generation of somatic motor neurons was affected in a way that is very comparable to what was observed in *Pax6*^{Sey} mutant mice. While these findings support the hypothesis that mainly the PAI PD sub-domain is involved in patterning events that direct motor neuron generation within the hindbrain, it still needs to be elucidated whether the PAI domain redundantly compensates for loss of RED PD sub-domain function in Pax6^{Leca2} mutant embryos, or whether the RED sub-domain is not involved at all in cross-repressive interaction with Nkx2.2. Intriguingly, in embryos where either Pax6 PD sub-domain was selectively mutated, we observed normal generation of V1 and V2 interneurons within the hindbrain, which is in stark contrast to what was observed in *Pax6*^{Sey} mutant embryos, or the expansion of the p2 domain and increased generation of V2 interneurons at brachial levels in embryos where the Pax6 PAI PD sub-domain was mutated. Thus, while our findings reveal a negligible, if any role for the RED PD sub-domain during motor

progenitor zone formation, it appears that either PD sub-domain is sufficient to induce faithful ventral interneuron generation within the vertebrate hindbrain.

Exit point designation of hindbrain somatic motor axons is defective in Pax6 mutant embryos

Analyses of wholemount embryo preparations of *Pax6*^{Leca2}, *Pax6*^{Leca4} and *Pax6*^{Sey} mutant embryos revealed Hb9::eGFP positive fibers in the spinal accessory nerve (SAN) that is a pure bMN nerve (Guthrie, 2007). In *Pax6*^{Sey} mutants and upon selective mutation of the PAI PD sub-domain, sMN change their fate into bMN due to altered patterning of the p3 and pMN progenitor domains (Ericson et al., 1997b). However, at no time point, Hb9::eGFP is expressed in these motor neurons, and in *Pax6*^{Leca2} mutants generation of these neuronal subsets was not affected at all, thus arguing for a different origin of these "somatic" motor fibers: either sMN mismigrate to more dorsal positions in the neural tube and exit the neural tube at the wrong place, or somatic motor projections are misguided within the spinal cord to dorsal positions where normally branchio- and visceromotor axons leave the hindbrain. Indeed, we found that the latter option is true: somatic motor neurons reside at their ventral positions within the neural tube, however, in all three *Pax6* mutant lines, aberrant projections towards dorsal exit points were observed. Expression of the G-protein coupled receptor Cxcr4 was shown to enable somatic motor axons to identify their ventral exit points from the neural tube by interaction with its cytokine ligand Cxcl12 that is secreted by mesenchymal cells flanking the spinal cord and caudal hindbrain. Mutation of either receptor or ligand results in a similar phenotype as we observed in *Pax6* mutant embryos: Hb9::eGFP^{+} somatic motor axons projected to dorsal positions and left the neural tube vial dorsal exit points (Lieberam et al., 2005). Interestingly, microarray analysis performed on cerebral cortices of *Pax6*^{Sey}, *Pax6*^{Leca2} and *Pax6*^{Leca4} revealed differential expression of either Cxcl12 directly, or one of the two Cxcl12-receptors, namely Cxcr7. A distinctive feature of Cxcr7 is its high affinity for Cxcl12 and its ability to mediate efficient uptake and degradation of Cxcl12. Since Cxcr4 is rapidly degraded upon binding to Cxcl12, co-expression of Cxcr7 as a decoy receptor strongly influences Cxcl12-Cxcr4 dependent guidance: e.g.,

expression of Cxcr7 by non-migratory cells helps to shape chemokine gradients, or, in its function as decoy receptor, Cxcr7 is involved in sustaining responsiveness of the Cxcr4 pathway by preventing excessive degradation (Boldajipour et al., 2008; Haege et al., 2012; Hoffmann et al., 2012; Sánchez-Alcañiz et al., 2011). Up-regulation of Cxcr7, as observed in *Pax6*^{Leca4} mutant cortices, thus may effectively prevent Cxcl12 from binding to Cxcr4 and ultimately result in the same axon guidance phenotype as down-regulation of Cxcl12, which was observed in *Pax6*^{Leca2} mutant cortices (Walcher et al., 2013). It is thus possible that the two Pax6 PD sub-domains are differentially involved in the regulation of the Cxcl12-Cxcr4 system at hindbrain-levels. Investigations of earlier time points (E9.5) are therefore required to critically analyze expression the patterns of receptor-ligand systems involved in exit point designation.

p3-pMN boundary formation is established normally upon mutation of the PD sub-domains at brachial levels

While the importance of Pax6 for neuronal specification in the hindbrain has been extensively demonstrated, it is still poorly understood how Pax6 affects the generation of motor and interneurons at brachial spinal levels. A study by Lei et al., investigating downstream factors of Pax6 signaling to establish faithful boundary formation between the p3 and the pMN domain revealed that Pax6 inhibits expression of *Nkx2.2* in sMN progenitors by regulating the spatially restricted expression of the extracellular Wnt-inhibitor *sFRP2*, and *Tcf4,* which is a mediator of canonical Wnt-signaling in the pMN domain. Loss of *sFRP2* results in similar patterning defects as in *Pax6*^{Sey} mutant embryos with a dorsal expansion of the p3 domain. In embryos harboring the functional Null allele of *Pax6, sFRP2* is lost, and *Tcf4* is downregulated in the ventral spinal cord, arguing that Pax6 controls ventral patterning by regulating Wnt signaling status in neuronal progenitors (Hurlstone and Clevers, 2002; Kawano and Kypta, 2003; Lei et al., 2006). Interestingly, previous investigations by Li and colleagues revealed a diminishing importance for Pax6 itself for faithful patterning of progenitor zones in the ventral spinal cord according with the rostro-caudal position of the spinal cord: While at brachial positions the p3 domain is still enlarged, Sp8 was at least partially downregulated, and the pMN domain is diminished, progenitor zones are established largely normal at

lumbar and sacral levels in *Pax6*^{Sey} mutant embryos. Only upon additional removal of Sp8, a similar expansion of the p3 domain at the expense of the pMN domain could be observed within the caudal spinal cord (Fig. 8A – D, Li et al., 2014). These findings coincide with observations of embryos where *sFRP2* was eliminated, and a dorsal expansion of the p3 domain was also observed at lumbar levels (Lei et al., 2006). Intriguingly, in embryos where the Pax6 PD sub-domains were mutated selectively, the p3 domain was established normally, suggesting that the signaling pathways containing *Nkx2.2* expression in pMN progenitor cells are still functioning. Indeed, Sp8 has been identified only recently to be Wnt-responsive (Dunty et al., 2014), arguing for a redundant function for both PAI and RED sub-domains for regulation of Wnt-signaling at the p3-pMN border at brachial levels to establish proper progenitor cell patterning in collaboration with Sp8. Further investigations concerning *Sp8* expression in *sFRP2* mutant mice and combinatorial elimination of Sp8 together with either the PAI or RED Pax6 PD sub-domains are required to determine the molecular mechanisms for correct boundary formation (Lei et al., 2006; Treichel et al., 2003).

Pax6 is essential for the generation of MMC and late born LMCl motor neurons

Interestingly, generation of specific motor neuron subsets was affected in both *Pax6*^{Sey} and *Pax*^{Leca4} mutant embryos. LIM homeodomain protein function is required to establish both the generic and columnar identities of motor neurons: Isl1 function, for example is required for the generation of all motor neurons (Pfaff et al., 1996), while Lhx3 and Lhx4 have more selective roles in the specification of motor neuron columnar identity (Sharma et al., 1998). Within the hindbrain, all sMN can be identified by the combined expression of these transcription factors, while at spinal levels, MMC neurons innervating axial musculature retain expression of Lhx3 and Lhx4 (Kania et al., 2000). In both mouse lines, this motor neuron population is decreased in cell numbers, which, however, might be caused by different reasons: In *Pax6*^{Sey} mutant embryos an expanded p3 domain suggests a fate change towards V3 interneurons. In *Pax6*^{Leca4} mutant embryos, V3 interneurons are generated at normal numbers, arguing against a motor neuron to V3 interneuron switch. One interesting fact that both lines share is that

Pax6, or more specifically the Pax6 PAI PD sub-domain impacts on generation of a subset of MMC motor neurons that express $Lim3^{+}/Isl1^{+}/Sp8^{+}$. Therefore it is likely, that to a certain extent not only an expanded p3 domain is responsible for the loss of MMC neurons, but rather interaction of Pax6 with Sp8 via the PAI domain is essential for the generation of these specific MMC neurons. Interestingly, also for MMC neuron generation, the Wnt-signaling pathway was shown to play a critical role. *Wnt4* is highly expressed in the p3 domain and facilitates MMC neuron generation from the most ventrally positioned $Olig2^{+}$ progenitor cells in the pMN domain. In $Wnt4^{-/-}$ mutant mice, generation of MMC motor neurons is significantly diminished, switching fate to columnar generated motor neurons, e.g. motor neurons of the hypaxial motor column at thoracic levels (Agalliu et al., 2009). Whether expression of *Wnt4* is affected in $Pax6^{Sey}$ and $Pax6^{Leca4}$ mutant embryos still needs to be elucidated

Next to molecular features, also differences in cell cycle exit further determine the sub-columnar identities of motor neurons: motor neurons that will form the medial aspect of the LMC leave the cell cycle before motor neurons of the prospective LMCl that have to migrate past the LMCm neurons to their final positions in the lateral ventral spinal cord. Secretion of Raldh2 by the early born motor neurons initiates down-regulation of Lhx3 and Isl1 in motor neurons of the LMCl, and activates Lim1 that controls growth of LMCl axons towards dorsal limb musculature (Kania et al., 2000). In both $Pax6^{Sey}$ and $Pax6^{Leca4}$ mutant embryos, total numbers of neurons of the LMC are not affected, however, proportions are shifted from the lateral towards the medial LMC. In accordance with this, projections to dorsal limb musculature were markedly thinned in these animals. Whether this shift is a result of diminished generation of only the LMCl sub-population of LMC motor neurons, or whether MMC motor neurons undergo a similar switch from non-columnar MMC to columnar LMCm motor neurons at brachial levels as observed for thoracic HMC neurons in $Wnt4^{-/-}$ mutant mice, and thus may compensate for a loss of this specific motor neuron subtype still needs to be elucidated.

Previous studies report, that while motor neuron generation is delayed and/or severely diminished in $Pax6^{Sey}$ mutant embryos, generation of oligodendrocyte precursors from the ventral-most compartment of the pMN domain is only slightly retarded during early oligodendrocyte generation (E13.5), and indistinguishable from the

wildtype situation at later stages (E18.5; Sun et al., 1998). In both *Pax6*^{Sey} and *Pax6*^{Leca4} mutant embryos, a subset of Olig2^{+} precursors are still present, their very ventral position arguing for oligodendrocyte precursor generation from this specific subset of cells. Furthermore, it has been established that Reelin^{+} and Slit1^{+} astrocytes are generated in response to combinatorial activity of Pax6 and Nkx6.1, respectively. While loss of *Pax6* causes loss of Reelin^{+} astrocytes, other astrocyte populations exhibited aberrant proliferation patterns and immature differentiation, thus inhibiting astrocyte maturation (Hochstim et al., 2008; Sakurai and Osumi, 2008). Analyses of embryos in which the respective Pax6 PD sub-domains were mutated will substantially contribute to further dissect the molecular mechanisms of Pax6 activity and the structure-function relationships of this protein according to glia cell generation.

The Pax6 PAI PD sub-domain facilitates pMN-p2 progenitor domain patterning at brachial spinal levels

In contrast to observations in *Pax6*^{Sey} mutant embryos, generation of V3 and V1 interneurons at brachial levels is taking place normally in embryos where either the PAI or the RED PD sub-domains are mutated. While at hindbrain levels specifically the PAI domain is still involved in correct patterning of the p3 and pMN progenitor domains, interneuron generation from the p2 and p1 domains seems to be mediated redundantly by both sub-domains at cranial levels. Intriguingly, though, while this appears to be the case also for the p3 and p1 domains in the brachial neural tube, patterning of the p2 domain is particularly altered upon selective mutation of the PAI PD sub-domain. In embryos with a functional Null allele of Pax6, this domain is slightly diminished and gives rise to fewer interneurons, which results from a lack of activation of the direct Pax6 target gene *Ngn2* which plays a critical role for induction of V2 interneuron generation, and its loss recapitulates diminished generation or lack of motor and interneurons already observed upon mutation of *Pax6* (Bel-Vialar et al., 2007; Scardigli et al., 2001). At least three different enhancers regulate the expression of *Ngn2,* and their dorso-ventral expression-pattern is critically involved in the coordination of homeodomain transcription factors involved in neuronal subtype generation within the ventral spinal

cord. Enhancer E1, e.g. is important for the generation of V1 interneurons, and is lost in *Pax6*^{Sey} mutant embryos, while the domains containing the E2 and E3 enhancers which are involved in V3, V2, and motor neuron generation were enlarged upon loss of *Pax6* (Scardigli et al., 2001). Furthermore, the phosphorylation status of Ngn2 at two specific serine residues is of critical importance for the interaction with LIM homeodomain transcription factors to generate motor neurons, while in its unphosphorylated state, Ngn2 promotes V2 interneuron generation (Ma et al., 2008). However, it still needs to be determined whether mispatterning of progenitor zones holds responsible for aberrant generation of neuronal populations in the ventral spinal cord, or if also post-translational modifications are involved. Interestingly, when compared to selective mutation of the PAI PD sub-domain, various phenotypes look most severe or opposite in *Pax6*^{Sey} mutant embryos. Depending on which truncated form of Pax6 is present in the analyzed animals, nonsense-mediated decay or rapid protein degradation take place, effectively preventing binding of mutated Pax6 to its respective binding sites (Numayama-Tsuruta et al., 2007; Tzoulaki et al., 2005). In the *Pax6*^{Sey} mutant mouse line, which was determined to harbor a functional Null allele (Ramaesh et al., 2009), however, truncated protein is still detectable (Numayama-Tsuruta et al., 2007), thus, it is likely that the remaining PD binds to its respective targets, however, is unable to properly interact with other proteins due to the lack of the remaining domains, thus acting as a dominant negative. In *Pax6*^{Leca2} and *Pax6*^{Leca4} mutant embryos, the respective PAI and RED sub-domains of the Pax6 PD were selectively mutated, while all other domains are still functional, thus enabling other protein-protein and protein-DNA interactions, in the case of *Ngn2* also driving generation of neurons (Lee et al., 2005). Upon mutation of the PAI PD sub-domain, we found that *Ngn2* is still highly expressed in the ventricular zone, arguing for alterations in the reciprocal regulation of *Pax6* and *Ngn2* expression and maintenance in the spinal cord, which very likely affects both progenitor cell proliferation and differentiation to mature neurons (Bel-Vialar et al., 2007; Scardigli et al., 2001). This, and the fact that both PAI and RED sub-domains may compensate to a certain extent for the loss of the other domain very likely account for the fact that various phenotypes look most severe (e.g. missing V1 interneurons) or opposite (increased levels of V2 interneurons) in the *Pax6*^{Sey} mutant mouse line.

Thus, our findings indicate selective roles of the Pax6 PAI PD sub-domain during patterning events of neuronal progenitor domains that are distinct at different levels within the neural tube. While at cranial levels it regulates boundary formation between the p3 and pMN domain, at brachial levels increase of V2 interneurons implicates a selective involvement of the PAI PD sub-domain for the correct establishment of the patterning of the pMN and p2 domains. Interestingly, the RED PD sub-domain, while not playing a role for neuronal generation at either level within the neural tube, affects axonal pathfinding of hypoglossal axons within the hindbrain.

Acknowledgements:

We thank J. Maetsch and A. Schaub for technical assistance. Sincere thanks go to N. Prakash and M. Xiang for providing plasmids for riboprobe generation. We gratefully acknowledge W. Wurst for supporting this project with fruitful scientific discussions from the beginning onwards, as well as the members of the Huber laboratory for helpful comments on the manuscript and discussions.

References

Agalliu, D., Takada, S., Agalliu, I., McMahon, A.P., Jessell, T.M., 2009. Motor neurons with axial muscle projections specified by Wnt4/5 signaling. Neuron 61, 708-720.

Alaynick, W.A., Jessell, T.M., Pfaff, S.L., 2011. SnapShot: spinal cord development. Cell 146, 178-178 e171.

Bel-Vialar, S., Medevielle, F., Pituello, F., 2007. The on/off of Pax6 controls the tempo of neuronal differentiation in the developing spinal cord. Developmental biology 305, 659-673.

Bertrand, N., Castro, D.S., Guillemot, F., 2002. Proneural genes and the specification of neural cell types. Nature reviews. Neuroscience 3, 517-530.

Bishop, K.M., Rubenstein, J.L., O'Leary, D.D., 2002. Distinct actions of Emx1, Emx2, and Pax6 in regulating the specification of areas in the developing neocortex. The Journal of neuroscience : the official journal of the Society for Neuroscience 22, 7627-7638.

Boldajipour, B., Mahabaleshwar, H., Kardash, E., Reichman-Fried, M., Blaser, H., Minina, S., Wilson, D., Xu, Q., Raz, E., 2008. Control of Chemokine-Guided Cell Migration by Ligand Sequestration. Cell 132, 463-473.

Briscoe, J., Pierani, A., Jessell, T.M., Ericson, J., 2000. A homeodomain protein code specifies progenitor cell identity and neuronal fate in the ventral neural tube. Cell 101, 435-445.

Briscoe, J., Sussel, L., Serup, P., Hartigan-O'Connor, D., Jessell, T.M., Rubenstein, J.L., Ericson, J., 1999. Homeobox gene Nkx2.2 and specification of neuronal identity by graded Sonic hedgehog signalling. Nature 398, 622-627.

Brunet, J.-F., Pattyn, A., 2002. Phox2 genes — from patterning to connectivity. Current opinion in genetics & development 12, 435-440.

Crone, S.A., Quinlan, K.A., Zagoraiou, L., Droho, S., Restrepo, C.E., Lundfald, L., Endo, T., Setlak, J., Jessell, T.M., Kiehn, O., Sharma, K., 2008. Genetic Ablation of V2a Ipsilateral Interneurons Disrupts Left-Right Locomotor Coordination in Mammalian Spinal Cord. Neuron 60, 70-83.

Del Barrio, M.G., Taveira-Marques, R., Muroyama, Y., Yuk, D.I., Li, S., Wines-Samuelson, M., Shen, J., Smith, H.K., Xiang, M., Rowitch, D., Richardson, W.D., 2007. A regulatory network involving Foxn4, Mash1 and delta-like 4/Notch1 generates V2a and V2b spinal interneurons from a common progenitor pool. Development 134, 3427-3436.

Dunty, W.C., Jr., Kennedy, M.W., Chalamalasetty, R.B., Campbell, K., Yamaguchi, T.P., 2014. Transcriptional profiling of Wnt3a mutants identifies Sp transcription factors as essential effectors of the Wnt/beta-catenin pathway in neuromesodermal stem cells. PloS one 9, e87018.

Epstein, J.A., Glaser, T., Cai, J., Jepeal, L., Walton, D.S., Maas, R.L., 1994. Two independent and interactive DNA-binding subdomains of the Pax6 paired domain are regulated by alternative splicing. Genes Dev 8, 2022-2034.

Ericson, J., Briscoe, J., Rashbass, P., van Heyningen, V., Jessell, T.M., 1997a. Graded sonic hedgehog signaling and the specification of cell fate in the ventral neural tube. Cold Spring Harb Symp Quant Biol 62, 451-466.

Ericson, J., Rashbass, P., Schedl, A., Brenner-Morton, S., Kawakami, A., van Heyningen, V., Jessell, T.M., Briscoe, J., 1997b. Pax6 controls progenitor cell identity and neuronal fate in response to graded Shh signaling. Cell 90, 169-180.

Farah, M.H., Olson, J.M., Sucic, H.B., Hume, R.I., Tapscott, S.J., Turner, D.L., 2000. Generation of neurons by transient expression of neural bHLH proteins in mammalian cells. Development 127, 693-702.

Gehring, W.J., 1996. The master control gene for morphogenesis and evolution of the eye. Genes Cells 1, 11-15.

Götz, M., Stoykova, A., Gruss, P., 1998. Pax6 Controls Radial Glia Differentiation in the Cerebral Cortex. Neuron 21, 1031-1044.

Goulding, M., 2009. Circuits controlling vertebrate locomotion: moving in a new direction. Nature reviews. Neuroscience 10, 507-518.

Goulding, M., Pfaff, S.L., 2005. Development of circuits that generate simple rhythmic behaviors in vertebrates. Current opinion in neurobiology 15, 14-20.

Guthrie, S., 2007. Patterning and axon guidance of cranial motor neurons. Nature reviews. Neuroscience 8, 859-871.

Haege, S., Einer, C., Thiele, S., Mueller, W., Nietzsche, S., Lupp, A., Mackay, F., Schulz, S., Stumm, R., 2012. CXC chemokine receptor 7 (CXCR7) regulates CXCR4 protein expression and capillary tuft development in mouse kidney. PloS one 7, e42814.

Haubst, N., Berger, J., Radjendirane, V., Graw, J., Favor, J., Saunders, G.F., Stoykova, A., Gotz, M., 2004. Molecular dissection of Pax6 function: the specific roles of the paired domain and homeodomain in brain development. Development 131, 6131-6140.

Hever, A.M., Williamson, K.A., van Heyningen, V., 2006. Developmental malformations of the eye: the role of PAX6, SOX2 and OTX2. Clinical genetics 69, 459-470.

Hill, R.E., Favor, J., Hogan, B.L., Ton, C.C., Saunders, G.F., Hanson, I.M., Prosser, J., Jordan, T., Hastie, N.D., van Heyningen, V., 1991. Mouse small eye results from mutations in a paired-like homeobox-containing gene. Nature 354, 522-525.

Hochstim, C., Deneen, B., Lukaszewicz, A., Zhou, Q., Anderson, D.J., 2008. Identification of positionally distinct astrocyte subtypes whose identities are specified by a homeodomain code. Cell 133, 510-522.

Hoffmann, F., Muller, W., Schutz, D., Penfold, M.E., Wong, Y.H., Schulz, S., Stumm, R., 2012. Rapid uptake and degradation of CXCL12 depend on CXCR7 carboxyl-terminal serine/threonine residues. J Biol Chem 287, 28362-28377.

Huber, A.B., Kania, A., Tran, T.S., Gu, C., De Marco Garcia, N., Lieberam, I., Johnson, D., Jessell, T.M., Ginty, D.D., Kolodkin, A.L., 2005. Distinct roles for secreted semaphorin signaling in spinal motor axon guidance. Neuron 48, 949-964.

Huettl, R.E., Huber, A.B., 2011. Cranial nerve fasciculation and Schwann cell migration are impaired after loss of Npn-1. Developmental biology.

Huettl, R.E., Soellner, H., Bianchi, E., Novitch, B.G., Huber, A.B., 2011. Npn-1 contributes to axon-axon interactions that differentially control sensory and motor innervation of the limb. PLoS biology 9, e1001020.

Hurlstone, A., Clevers, H., 2002. T-cell factors: turn-ons and turn-offs. EMBO J 21, 2303-2311.

Jessell, T.M., 2000. Neuronal specification in the spinal cord: inductive signals and transcriptional codes. Nature reviews. Genetics 1, 20-29.

Kania, A., Johnson, R.L., Jessell, T.M., 2000. Coordinate roles for LIM homeobox genes in directing the dorsoventral trajectory of motor axons in the vertebrate limb. Cell 102, 161-173.

Kawano, Y., Kypta, R., 2003. Secreted antagonists of the Wnt signalling pathway. Journal of cell science 116, 2627-2634.

Lee, S.-K., Lee, B., Ruiz, E.C., Pfaff, S.L., 2005. Olig2 and Ngn2 function in opposition to modulate gene expression in motor neuron progenitor cells. Genes & Development 19, 282-294.

Lei, Q., Jeong, Y., Misra, K., Li, S., Zelman, A.K., Epstein, D.J., Matise, M.P., 2006. Wnt signaling inhibitors regulate the transcriptional response to morphogenetic Shh-Gli signaling in the neural tube. Developmental cell 11, 325-337.

Li, X., Liu, Z., Qiu, M., Yang, Z., 2014. Sp8 plays a supplementary role to Pax6 in establishing the pMN/p3 domain boundary in the spinal cord. Development.

Lieberam, I., Agalliu, D., Nagasawa, T., Ericson, J., Jessell, T.M., 2005. A Cxcl12-CXCR4 chemokine signaling pathway defines the initial trajectory of mammalian motor axons. Neuron 47, 667-679.

Ma, Y.-C., Song, M.-R., Park, J.P., Henry Ho, H.-Y., Hu, L., Kurtev, M.V., Zieg, J., Ma, Q., Pfaff, S.L., Greenberg, M.E., 2008. Regulation of Motor Neuron Specification by Phosphorylation of Neurogenin 2. Neuron 58, 65-77.

Ninkovic, J., Pinto, L., Petricca, S., Lepier, A., Sun, J., Rieger, M.A., Schroeder, T., Cvekl, A., Favor, J., Götz, M., 2010. The Transcription Factor Pax6 Regulates Survival of Dopaminergic Olfactory Bulb Neurons via Crystallin αA. Neuron 68, 682-694.

Numayama-Tsuruta, K., Arai, Y., Osumi, N., 2007. The small eye homozygote (rSey2/rSey2) can be regarded as a Pax6 null mutant. Imperial College Press, London.

Osumi, N., Hirota, A., Ohuchi, H., Nakafuku, M., Iimura, T., Kuratani, S., Fujiwara, M., Noji, S., Eto, K., 1997. Pax-6 is involved in the specification of hindbrain motor neuron subtype. Development 124, 2961-2972.

Palmesino, E., Rousso, D.L., Kao, T.J., Klar, A., Laufer, E., Uemura, O., Okamoto, H., Novitch, B.G., Kania, A., 2010. Foxp1 and lhx1 coordinate motor neuron migration with axon trajectory choice by gating Reelin signalling. PLoS biology 8, e1000446.

Pattyn, A., Vallstedt, A., Dias, J.M., Sander, M., Ericson, J., 2003. Complementary roles for Nkx6 and Nkx2 class proteins in the establishment of motoneuron identity in the hindbrain. Development 130, 4149-4159.

Pfaff, S.L., Mendelsohn, M., Stewart, C.L., Edlund, T., Jessell, T.M., 1996. Requirement for LIM homeobox gene Isl1 in motor neuron generation reveals a motor neuron-dependent step in interneuron differentiation. Cell 84, 309-320.

Quinones, H.I., Savage, T.K., Battiste, J., Johnson, J.E., 2010. Neurogenin 1 (Neurog1) expression in the ventral neural tube is mediated by a distinct enhancer and preferentially marks ventral interneuron lineages. Developmental biology 340, 283-292.

Ramaesh, T., Williams, S.E., Paul, C., Ramaesh, K., Dhillon, B., West, J.D., 2009. Histopathological characterisation of effects of the mouse Pax6(Leca4) missense mutation on eye development. Experimental eye research 89, 263-273.

Sakurai, K., Osumi, N., 2008. The neurogenesis-controlling factor, Pax6, inhibits proliferation and promotes maturation in murine astrocytes. The Journal of neuroscience : the official journal of the Society for Neuroscience 28, 4604-4612.

Sánchez-Alcañiz, J.A., Haege, S., Mueller, W., Pla, R., Mackay, F., Schulz, S., López-Bendito, G., Stumm, R., Marín, O., 2011. Cxcr7 Controls Neuronal Migration by Regulating Chemokine Responsiveness. Neuron 69, 77-90.

Sander, M., Paydar, S., Ericson, J., Briscoe, J., Berber, E., German, M., Jessell, T.M., Rubenstein, J.L., 2000. Ventral neural patterning by Nkx homeobox genes: Nkx6.1 controls somatic motor neuron and ventral interneuron fates. Genes Dev 14, 2134-2139.

Scardigli, R., Schuurmans, C., Gradwohl, G., Guillemot, F., 2001. Crossregulation between Neurogenin2 and Pathways Specifying Neuronal Identity in the Spinal Cord. Neuron 31, 203-217.

Sharma, K., Sheng, H.Z., Lettieri, K., Li, H., Karavanov, A., Potter, S., Westphal, H., Pfaff, S.L., 1998. LIM homeodomain factors Lhx3 and Lhx4 assign subtype identities for motor neurons. Cell 95, 817-828.

Sun, T., Pringle, N.P., Hardy, A.P., Richardson, W.D., Smith, H.K., 1998. Pax6 Influences the Time and Site of Origin of Glial Precursors in the Ventral Neural Tube. Molecular and Cellular Neuroscience 12, 228-239.

Takahashi, M., Osumi, N., 2002. Pax6 regulates specification of ventral neurone subtypes in the hindbrain by establishing progenitor domains. Development 129, 1327-1338.

Thaung, C., West, K., Clark, B.J., McKie, L., Morgan, J.E., Arnold, K., Nolan, P.M., Peters, J., Hunter, A.J., Brown, S.D., Jackson, I.J., Cross, S.H., 2002. Novel ENU-induced eye mutations in the mouse: models for human eye disease. Human molecular genetics 11, 755-767.

Treichel, D., Schock, F., Jackle, H., Gruss, P., Mansouri, A., 2003. mBtd is required to maintain signaling during murine limb development. Genes Dev 17, 2630-2635.

Tzoulaki, I., White, I.M., Hanson, I.M., 2005. PAX6 mutations: genotype-phenotype correlations. BMC Genet 6, 27.

Walcher, T., Xie, Q., Sun, J., Irmler, M., Beckers, J., Ozturk, T., Niessing, D., Stoykova, A., Cvekl, A., Ninkovic, J., Gotz, M., 2013. Functional dissection of the paired domain of Pax6 reveals molecular mechanisms of coordinating neurogenesis and proliferation. Development 140, 1123-1136.

Wichterle, H., Lieberam, I., Porter, J.A., Jessell, T.M., 2002. Directed differentiation of embryonic stem cells into motor neurons. Cell 110, 385-397.

Yang, X., Tomita, T., Wines-Samuelson, M., Beglopoulos, V., Tansey, M.G., Kopan, R., Shen, J., 2006. Notch1 signaling influences v2 interneuron and motor neuron development in the spinal cord. Developmental neuroscience 28, 102-117.

Tables

Position in the neural tube	*Pax6*^{Sey}	*Pax6*^{Leca4}	*Pax6*^{Leca2}
Abducens nucleus			
Progenitor domains	↑ p3; ↓ pMN *	↑ p3; ↓ pMN	No alterations
Motor neurons	↑ bMN, vMN; ↓sMN *	↑ bMN, vMN; ↓sMN	No alterations
Peripheral projections	Abducens nerve absent	Abducens nerve absent	No alterations
Interneurons	V1 and V2 not established **	No alterations	No alterations
Hypoglossal nucleus			
Progenitor domains	↑ p3; ↓ pMN *,**	↑ p3; ↓ pMN	No alterations
Motor neurons	↑ bMN, vMN; ↓sMN *,**	↑ bMN, vMN; ↓sMN	No alterations
Peripheral projections	Hypoglossal nerve absent Aberrant somatic motor projections in the SAN	Hypoglossal nerve largely reduced Aberrant somatic motor projections in the SAN	Hypoglossal nerve normal Aberrant somatic motor projections in the SAN
Interneurons	V1 and V2 not established *	No alterations	No alterations
Brachial level			
Progenitor domains	↑ p3; ↓ pMN; ↓ p2	p3 normal; ↓ pMN; ↑ p2	No alterations
Motor neurons	↓ MMC; ↓LMCl	↓ MMC; ↓LMCl	No alterations
Peripheral projections	Thinned intercostal, msc and rad projections, reduced distal advancement	Thinned intercostal, msc and rad projections, distal advancement normal	No alterations
Interneurons	↓ V1; ↓ V2a/b/c; ↑ V3	V1 normal; ↑ V2a/b; V2c normal; V3 normal	No alterations

Table 1: Summary of phenotypes observed in *Pax6*^{Sey}, *Pax6*^{Leca4} and *Pax6*^{Leca2} mutant embryos.

* Ericson et al., 1997b

** Osumi et al., 1997

Figure Legends

Figure 1: Mutation of the PAI domain and the functional Null allele of Pax6 impair formation of cranial somatic motor nerves.

Fluorescent immunohistochemistry against Hb9::eGFP (green, somatic motor nerves) and neurofilament (red, all motor and sensory projections) on wholemount embryo preparations. **(A)** Schematic illustration of the domain structure of Pax6. **(B)** Schematic illustration of cranial nerves with abducens (green, magenta box) and hypoglossal (green, blue box) projections. **(C, D)** Somatic motor axons of the abducens nucleus leave the neural tube at E10.5 in control and *Pax6*^{Leca2} mutant embryos and have formed a distinct trajectory towards the eye by E11.5 **(C', D')**. **(E – G)** In *Pax6*^{Leca4} and *Pax6*^{Sey} mutant embryos, abducens projections are severely reduced or absent from the hindbrain ($p^{Leca4\ E10.5} \leq 0.0008$, $p^{Leca4\ E11.5} \leq 0.0001$; $p^{Sey\ E10.5} \leq 0.0008$, $p^{Sey\ E11.5} \leq 0.0002$). **(H – I')** Somatic motor rootlets from the hypoglossal nucleus have formed the hypoglossal projection targeting the tongue muscle in control and *Pax6*^{Leca2} mutant embryos. **(J, J', L, M)** The number of hypoglossal rootlets and hypoglossal nerve thickness at the point where all rootlets have converged (CP, arrow) is severely reduced in *Pax6*^{Leca4} mutant embryos when compared to control littermates (rootlets: $p^{Leca4\ E10.5} \leq 0.0002$, $p^{Leca4\ E11.5} \leq 0.003$; thickness at CP: $p^{Leca4\ E10.5} \leq 0.0005$, $p^{Leca4\ E11.5} \leq 0.002$). **(K, K', L, M)** Hypoglossal projections are largely absent from *Pax6*^{Sey} mutant embryos' hindbrains and do not reach the CP (arrow, rootlets: $p^{Sey\ E10.5} \leq 0.002$, $p^{Sey\ E11.5} \leq 0.0004$). Arrowheads in **I', J'** and **K'** indicate aberrant somatic projections in the spinal accessory nerve observed in all three Pax6 mutants. **Abbreviations:** BAs= branchial (pharyngeal) arches, C1= first cervical spinal nerve, V= trigeminal ganglion with ophthalmic, maxillary and mandibular branches, VI= abducens nerve, VII/VIII= facial and vestibulocochlear nerve, IX= glossopharyngeal nerve, X= vagus nerve, XI= spinal accessory nerve, XII= hypoglossal nerve. Scale bar in J' equals 150µm for all panels.

Figure 2: Mutation of the PAI domain impacts on p3-pMN progenitor zone boundary formation.

Hb9::eGFP demarcates somatic motor neurons in the abducens and the hypoglossal nucleus. Fluorescent immunohistochemistry against Nkx2.2 and Olig2 labels neuronal progenitors in the p3 and the pMN domain, respectively. **(B – D')** In *Pax6*^{Leca2} mutant embryos, size and number of Nkx2.2^{+} cells within the p3 domain at both abducens and hypoglossal levels were not altered when compared to control littermates at E10.5 and E11.5 **(A – B', G, H)**. Olig2^{+} motor neuron progenitors in the pMN domain are generated at normal numbers **(I)**. **(E – F', G – I)** In *Pax6*^{Leca4} mutant embryos, the p3 domain is enlarged at the level of the abducens and the hypoglossal nucleus while somatic motor neuron progenitors of the pMN domain are loosely dispersed in between Nkx2.2^{+} cells and significantly reduced in number when compared to littermate controls (abducens level: size p3 domain: E10.5: 118.6 µm ± 11.23 vs. 60.18 µm ± 5.15, p≤ 0.01; E11.5: 103.8 µm ± 13.99 vs. 58.38 µm ± 1.27, p≤ 0.04; number of Nkx2.2^{+} cells: E10.5: 62.81 ± 6.70 vs. 36.53 ± 3.67 p≤ 0.01; E11.5: 51.75 ± 2.91 vs. 31.50 ± 3.11, p≤ 0.03; number of Olig2^{+} progenitors: E10.5: 6.59 ± 1.47 vs. 14.77 ± 0.83, p≤ 0.002; E11.5: 2.36 ± 0.5 vs. 9.06 ± 1.53, p≤ 0.008. Hypoglossal level: size p3 domain: E10.5: 83.21 µm ± 4.97 vs. 53.95 µm ± 1.54, p≤ 0.0002; E11.5: 98.81 µm ± 3.13 vs. 54.96 µm ± 2.28, p≤ 0.008; number of Nkx2.2^{+} cells: E10.5: 61.88 ± 10.50 vs. 31.20 ± 1.49, p≤ 0.03; E11.5: 46.36 ± 2.57 vs. 30.36 ± 1.62, p≤ 0.006; number of Olig2^{+} progenitors: E10.5: 11.02 ± 0.88 vs. 18.72 ± 0.94, ≤ 0.002, E11.5: 7.30 ± 1.65 vs. 15.49 ± 0.82, p≤ 0.001). Scale bar in F' equals 50µm for all panels.

Figure 3: Branchio- and visceromotor neurons are generated on the expense of somatic motor neurons in *Pax6*^{Leca4} mutants.

Fluorescent immunohistochemistry against Phox2a visualizes bMN and vMN. *Hb9::eGFP* labels sMN. Immunohistochemistry against Chx10 and En1 shows V2a and V1 interneurons, respectively. Yellow dashed line demarcates midline of the neural tube. **(A – B', G)** bMN and vMN that are generated from progenitors of the p3 domain are established at normal numbers at both abducens and hypoglossal levels in *Pax6*^{Leca2} mutant embryos, when compared to littermate controls. Also generation of somatic motor neurons is not affected by mutation of the RED domain (*Hb9::eGFP*$^{+}$ in **D – E', G**). **(C, C', G)** In *Pax6*^{Leca4} mutant embryos, bMN and vMN numbers are increased

(abducens level: $p^{Leca4} \leq 0.009$; hypoglossal level: $p^{Leca4} \leq 0.0034$), while somatic motor neuron **(F, F')** numbers are decreased in number when compared to control littermates (abducens level: $p^{Leca4} \leq 0.02$; hypoglossal level: $p^{Leca4} \leq 0.04$). **(D –F', H)** Generation of $Chx10^+$ V2a and $En1^+$ V1 interneurons was not affected by either ablation of the PAI or the RED domain at both abducens and hypoglossal levels. **(I)** Schematic summary: Mutation of the RED domain in *Pax6*^{Leca2} mutant embryos does not affect progenitor zone or neuron generation. Similar to *Pax6*^{Sey} mutants, in *Pax6*^{Leca4} mutant embryos the p3 domain is enlarged on the expense of the pMN domain, however, generation of V2 and V1 interneurons is not affected. Scale bar in **F'** 75µm for **A – C'** and 30µm for **D – F'**.

Figure 4: Formation of dorsal limb innervation is impaired in *Pax6*^{Leca4} and *Pax6*^{Sey} mutant embryos.

Fluorescent immunohistochemistry against *Hb9::eGFP* (green, motor projections) and neurofilament (red, motor and sensory projections) on whole mount embryo preparations. **(A – E)** At E10.5, spinal nerves from the segments C4 – Th1 (1 – 6) have formed the brachial plexus in control littermates. In all three *Pax6* mouse lines, a normal brachial plexus was established. Quantification of a fasciculation coefficient shows normal formation of the six mixed sensory-motor spinal nerve projections that contribute to the brachial plexus. At E12.5, five specific nerve branches of which the motor sub-components innervate dorsal and ventral limb musculature are detectable in control embryos and have grown to specific positions within the developing limb **(F)**. **(G – I)** This general growth pattern is not altered in *Pax6*^{Leca2}, *Pax6*^{Leca4}, and *Pax6*^{Sey} mutant embryos, however, motor branches do not invade the forelimb as far as in control littermates in *Pax6*^{Sey} mutant embryos (**J**, $p^{Sey} \leq 0.002$). Quantification of the individual thickness of nerves revealed that the musculocutaneous nerve (msc), the first branch of the radial nerve (1), and the radial nerve (2) itself are significantly thinner in *Pax6*^{Leca4} mutant embryos when compared to control embryos ($p^{Leca4\ msc} \leq 0.02$, $p^{Leca4\ 1} \leq 0{,}03$ $p^{Leca4\ 2} \leq 0.006$). Median and ulnar projections are not altered in their individual thickness **(K)**. In *Pax6*^{Sey} mutant embryos, in 2/3 embryos the first branch of the radial nerve was missing ($p^{Sey\ 1} \leq 0.0004$). Furthermore, the radial nerve itself was significantly thinner

when compared to littermate controls ($p^{Sey\ 2} \leq 0.002$) and also the musculocutaneous nerve was reduced in thickness ($p^{Sey\ msc} \leq 0.01$). Median and ulnar projections were established normally. **Abbreviations**: msc= musculocutaneous nerve, 1= 1st branch of the radial nerve, 2= radial nerve, 3= median nerve, 4= ulnar nerve. Scale bar in **I** equals 150µm for **A – D**, and 400µm for **F – I**.

Figure 5: p3 and pMN progenitor zone formation and motor neuron generation at brachial levels.

(A) Schematic illustration of progenitor zones and motor neurons that innervate axial (MMC) or limb musculature (LMC) in the developing murine embryo. **(B – D')** In *Pax6*^{Leca2} and *Pax6*^{Leca4} mutant embryos, the p3 domain (Nkx2.2$^+$) is established at normal extensions and cell numbers when compared to control littermates **(F, G)**. At E10.5, motor neuron progenitors are generated at normal numbers in both Pax6 mutant lines, however, in *Pax6*^{Leca4} mutant embryos, a drop in Olig2$^+$ progenitor number at E11.5 ($p \leq 0.001$) was observed when compared to control embryos **(H)**. **(E – H)** In *Pax6*^{Sey} mutant embryos, the p3 domain is enlarged on the expense of the pMN domain ($p^{Sey\ size\ E10.5} \leq 0.002$, $p^{Sey\ number\ E10.5} \leq 0.002$; $p^{Sey\ size\ E11.5} \leq 0.003$, $p^{Sey\ number\ E11.5} \leq 0.001$), with reduced Olig2$^+$ motor neuron progenitors that are interspersed between Nkx2.2$^+$ cells ($p^{Sey\ E10.5} \leq 0.009$, $p^{Sey\ E11.5} \leq 0.0003$). **(I – L)** Fluorescent immunohistochemistry against FoxP1 (green) and Isl1 (red) labels motor neurons in the LMCl (FoxP1$^+$/Isl1$^-$) and LMCm (FoxP1$^+$/Isl1$^+$). Arrows in **K** and **L** point to the area in which the MMC is located and appears to be reduced in cell numbers. **(M)** By E12.5, motor neurons of the two sub-columns constitute equal proportions to the LMC. In *Pax6*^{Leca2} mutant embryos, proportions of motor neurons contributing to either the lateral or the medial aspect of the LMC were not significantly altered (LMCl: 0.47 ± 0.02, LMCm: 0.53 ± 0.02, n=4). In embryos where the PAI PD sub-domain was mutated or in *Pax6*^{Sey} mutant embryos, proportions of neurons contributing to the LMCm significantly exceed that of neurons contributing to the LMCl, when compared to littermate controls ($p^{Leca4} \leq 0.0006$, $p^{Sey} \leq 0.03$; $p^{LMCm\ ctrl/Leca4} \leq 0.004$, $p^{LMCl\ ctrl/Leca4} \leq 0.004$; $p^{LMCm\ ctrl/Sey} \leq 0.04$, $p^{LMCl\ Sey} \leq 0.04$). Scale bar in **L** equals 50µm for all panels.

Figure 6: p3/pMN boundary formation is intact upon selective mutation of the PAI PD sub-domains, while expression of *Ngns* is altered in *Pax6^{Leca4}* mutant embryos. **(A, B, E)** At E11.5, borders between Sp8^{+} and Nkx2.2^{+} progenitor cells are well defined in control embryos and *Pax6^{Leca2}* mutant embryos. Olig2^{+} motor neuron progenitors reside right at the border to the p3 domain, and cells are migrating out of the progenitor domain in comparable numbers **(**arrows in **A** and **B**, **F**). **(C, E, F)** In *Pax6^{Leca4}* mutant embryos, the border between the p3 and the pMN domain is established normally, however, the coefficient of the size of the domain containing Sp8^{+} cells normalized to the size of the spinal cord is enlarged into dorsal regions ($p^{Leca4} \leq 0.01$). Olig2^{+} cells in the pMN domain are reduced in number, and only very sparse Sp8^{+} cells leave the progenitor domain (arrows in **C**, $p^{Leca4} \leq 0.01$). **(D – F)** In *Pax6^{Sey}* mutant embryos, the size of the domain containing Sp8^{+} progenitors is not enlarged when compared to control embryos, however, the border between the p3 and pMN domain is not clearly circumvented: at the position where the pMN domain should reside, Sp8^{+} cells and Nxk2.2^{+} cells or the enlarged p3 domain overlap (bracket), while Olig2^{+} motor progenitors are largely absent. Also here, very few Sp8^{+} cells leave the progenitor domain (arrows in **D**, $p^{Sey} \leq 0.03$). **(A' – D'**, **G)** A closer investigation of MMC motor neurons (green dashed box in **A**) concerning expression of Sp8 revealed a significant decrease of Isl1^{+}/Lim3^{+}/Sp8^{+} cells in *Pax6^{Leca4}* ($p^{Leca4} \leq 0.007$) and *Pax6^{Sey}* ($p^{Sey} \leq 0.007$) mutant embryos, while no alterations were observed in *Pax6^{Leca2}* mutant embryos when compared to control littermates. **(H, I, K, L)** Expression of *Ngn1* was not altered upon mutation of the RED PD sub-domain or in embryos with a functional Null allele of *Pax6* when compared to littermate controls. In *Pax6^{Leca4}* mutant embryos, the domain expressing *Ngn1* was enlarged dorsally and the coefficient of the size of the domain containing *Ngn1*$^{+}$ cells normalized to the size of the spinal cord was significantly increased (**J**, **L**; $p^{Leca4} \leq 0.004$). **(M, N, O)** Also expression of *Ngn2* is elevated in embryos where the Pax6 PAI PD sub-domain was mutated, and explicitly also found within the pMN domain, while in control embryos and in *Pax6^{Leca2}* mutant embryos was not altered, and absent from the pMN domain. **(P)** Expression of *Ngn2* is absent from the pMN domain and downregulated in embryos with a functional Null allele of Pax6. Scale bar in **P** equals 50µm for **A – P**, and 20 µm for **A' – D'**.

Figure 7: Excessive numbers of V2a/b interneurons are generated in *Pax6^{Leca4}* mutant embryos.

(A) Schematic illustration of V1, V2, and V3 interneurons in the ventral spinal cord. **(B – F)** In *Pax6^{Leca4}* mutant embryos, Chx10^{+} interneurons are drastically increased at brachial levels ($p^{Leca4} \leq 0.0001$), while *Pax6^{Sey}* mutant embryos significantly less V2a interneurons were generated ($p^{Sey} \leq 0.007$). In *Pax6^{Leca2}* mutant embryos, normal numbers of V2a interneurons are generated, when compared to littermate controls. **(G – L)** Numbers of V2b interneurons (Gata2^{+}, green) are also generated at normal numbers in *Pax6^{Leca2}* mutants, while they are significantly increased in number in *Pax6^{Leca4}* mutant embryos ($p^{Leca4} = 0.006$), and decreased in number in *Pax6^{Sey}* mutant embryos when compared to littermate controls. V2c (Sox1^{+}, red) are established normally upon mutation of either the PAI or RED PD sub-domains, however, they are generated at lower numbers in *Pax6^{Sey}* mutant embryos ($p^{Sey} \leq 0.02$). **(M – Q)** V1 interneurons (*En1^{+}*) are generated in normal numbers in *Pax6^{Leca2}* and *Pax6^{Leca4}* mutant embryos, while they are completely absent in *Pax6^{Sey}* mutant embryos. **(R – V)** V3 interneurons (Sim1^{+}) are generated in normal numbers in *Pax6^{Leca2}* and *Pax6^{Leca4}* mutant embryos, while they are increased in number in *Pax6^{Sey}* mutant embryos ($p^{Sey} \leq 0.01$). Scale bar in **U** equals 50µm for all panels.

Figure 8: Schematic summary.

(A, B) Wildtype situation of progenitor zone patterning and neuron generation. **(C, D)** *Pax6^{Sey}* mutant embryos show an enlarged p3 domain on the expense pf the pMN domain with increased numbers of Nkx2.2^{+} progenitors and decreased motor and V2a interneuron progenitors. Accordingly, V3 interneurons are generated in elevated numbers, while specific subsets of MMC and LMCl neurons as well as V2 interneurons were generated in decreased numbers. V1 interneurons are missing completely. **(E, F)** Upon mutation of the RED domain, progenitor zone patterning and neuronal differentiation are not altered. **(G, H)** in *Pax6^{Leca4}* mutant embryos, the p3 and p1 and corresponding V3 and V1 interneurons are generated normally. The pMN domain is decreased by E11.5. Specific subsets of MMC and LMC motor neurons decreased. The

domain containing V2 interneuron progenitors is expanded and gives rise to markedly increased V2a and V2b interneurons, while V2c establishment was not altered and appears to depend on Pax6-independent mechanisms.

Figure S1: Quantification of abducens and hypoglossal projections.

(A) Quantification of axons contributing to the abducens nerve. **(B)** Determination of hypoglossal rootlets for quantification of projections contributing to the hypoglossal nerve.

Figure S2: Ectopic hypoglossal projections in Pax6 mutant embryos.

(A) In control embryos, hypoglossal projections (GFP^+) exit the neural tube at a ventral position (arrowhead). **(B – D)** In *Pax6*^{Leca2}; *Pax6*^{Leca4} and *Pax6*^{Sey} mutant embryos, GFP^+ axons project to dorsal positions in the neural tube and leave it at ectopic dorsal positions (arrows), joining the projection of the SAN (yellow dashed circle). Scale bar in **D** equals 50µm for all panels.

Figure S3: Formation of target specific branches at E11.5 is not impaired upon mutation of Pax6.

Fluorescent immunohistochemistry against *Hb9::eGFP* (green, motor projections) and Neurofilament (red, motor and sensory projections) on whole mount embryo preparations. **(A)** By E11.5, first target specific bundles that will innervate limb musculature have formed in control embryos (arrowheads). **(B – D)** Target specific branches are established normally in mice where either the RED or the PAI PD sub-domains were mutated, or in embryos with a functional Null allele of Pax6 (arrowheads). Scale bar in **D** equals 150µm for all panels.

Figure S4: LMC motor neurons at E10.5 and E11.5.

(A – E) At E10.5, motor neurons that will innervate the limb have not yet segregated into the lateral ($FoxP1^+/Isl1^-$) and the medial ($FoxP1^+/Isl1^+$) aspects of the LMC, respectively, but are rather interspersed. Later born neurons of the LMCl still migrate through the pool of LMCm neurons and comprise a lower proportion of the entire LMC. **(F – J)** By E11.5,

motor neurons of the LMCl (cyan dashed line) and LMCm (magenta dashed line) have settled at their respective positions within the LMC. Proportions are now equally distributed in control, *Pax6*^{Leca2} and *Pax6*^{Leca4} mutant embryos. In *Pax6*^{Sey} mutant embryos the proportion of neurons contributing to the medial aspect of the LMC is significantly higher than of neurons contributing to the LMCl ($p^{Sey} \leq 0.03$). Scale bar in **I** equals 50µm for **A – D**, and 40µm for **F – I**.

Figure S5: MMC motor neuron numbers and intercostal nerve thickness are reduced in *Pax6*^{Leca4} and *Pax6*^{Sey} mutant embryos.

(A – E) Immunohistochemical staining against Isl1 (red) and Lim 3 (green) reveals reduced numbers of MMC motor neurons in *Pax6*^{Leca4} ($p^{Leca4} \leq 0.001$) and *Pax6*^{Sey} mutant embryos ($p^{Sey} \leq 0.02$), while numbers in *Pax6*^{Leca2} mutant embryos were not altered when compared to littermate controls. **(F – N)** Quantification of intercostal nerve thickness shows that these projections are significantly thinner in *Pax6*^{Leca4} ($p^{Leca4\ E11.5} \leq 0.03$, $p^{Leca4\ E12.5} \leq 0.0001$) and *Pax6*^{Sey} ($p^{Sey\ E11.5} \leq 0.0006$, $p^{Sey\ E12.5} \leq 0.0001$) mutant embryos at E11.5 and E12.5, while thickness was not reduced in *Pax6*^{Leca2} mutant embryos when compared to control littermates. Scale bar in **M** equals 40µm for **A – D**, 100µm for **F – I**, and 200µm for **J – M**.

Figure S6: V2a/b progenitor numbers are increased in *Pax6*^{Leca4} mutant embryos.

(A) Schematic illustration of V2 interneuron generation. **(B – G)** Total numbers of Lim3$^+$ cells that in part give rise to V2a interneurons are drastically increased in number in *Pax6*^{Leca4} mutant embryos ($p^{Leca4\ \#Lim3} \leq 0.002$) and spread over a wider area close to the ventricular zone ($p^{Leca4\ size\ Lim3} \leq 0.0007$), while these parameters are not altered in *Pax6*^{Leca2} when compared to littermate controls. In *Pax6*^{Sey} mutant embryos the domain close to the ventricular zone containing Lim3$^+$ is significantly smaller ($p^{Sey\ size\ Lim3} \leq 0.0007$). More peripherally, these cells appear disorganized, but are not altered significantly in number. **(H – M)** Numbers of *Foxn4*$^+$ V2b progenitors and size of the progenitor domain are increased in *Pax6*^{Leca4} mutant embryos ($p^{Leca4\ size} \leq 0.0007$; $p^{Leca4\ number} \leq 0.001$), while they are not altered significantly in *Pax6*^{Leca2} and *Pax6*^{Sey} mutant embryos when compared to littermate controls. **(N – S)** Accordingly, numbers of Ascl1$^+$

V2b progenitors and size of the domain were increased in *Pax6*^{Leca4} mutant embryos ($p^{Leca4\ size} \leq 0.002$; $p^{Leca4\ number} = 0.005$), while they are not altered in *Pax6*^{Leca2} mutant embryos when compared to littermate controls. In *Pax6*^{Sey} mutant embryos, the size of the domain containing Ascl1^{+} progenitors was not changed ($p^{Sey\ size} \leq 0.15$), however, it contained significantly less Ascl1^{+} cells ($p^{Sey\ number} \leq 0.014$). Scale bar in **Q** equals 50m for all panels.

Figure S7: En1 expression is absent from spinal interneurons but not from other cell types in *Pax6*^{Sey} mutant embryos.

(A) In control embryos, expression of *En1* mRNA is evident in spinal interneurons (arrowheads) and lateral mesenchyme of the body (arrow). **(B)** In *Pax6*^{Sey} mutant embryos, *En1* expression is absent from interneurons within the spinal cord, while normal expression was observed in the body. Scale bar in **B** equals 50µm for all panels.

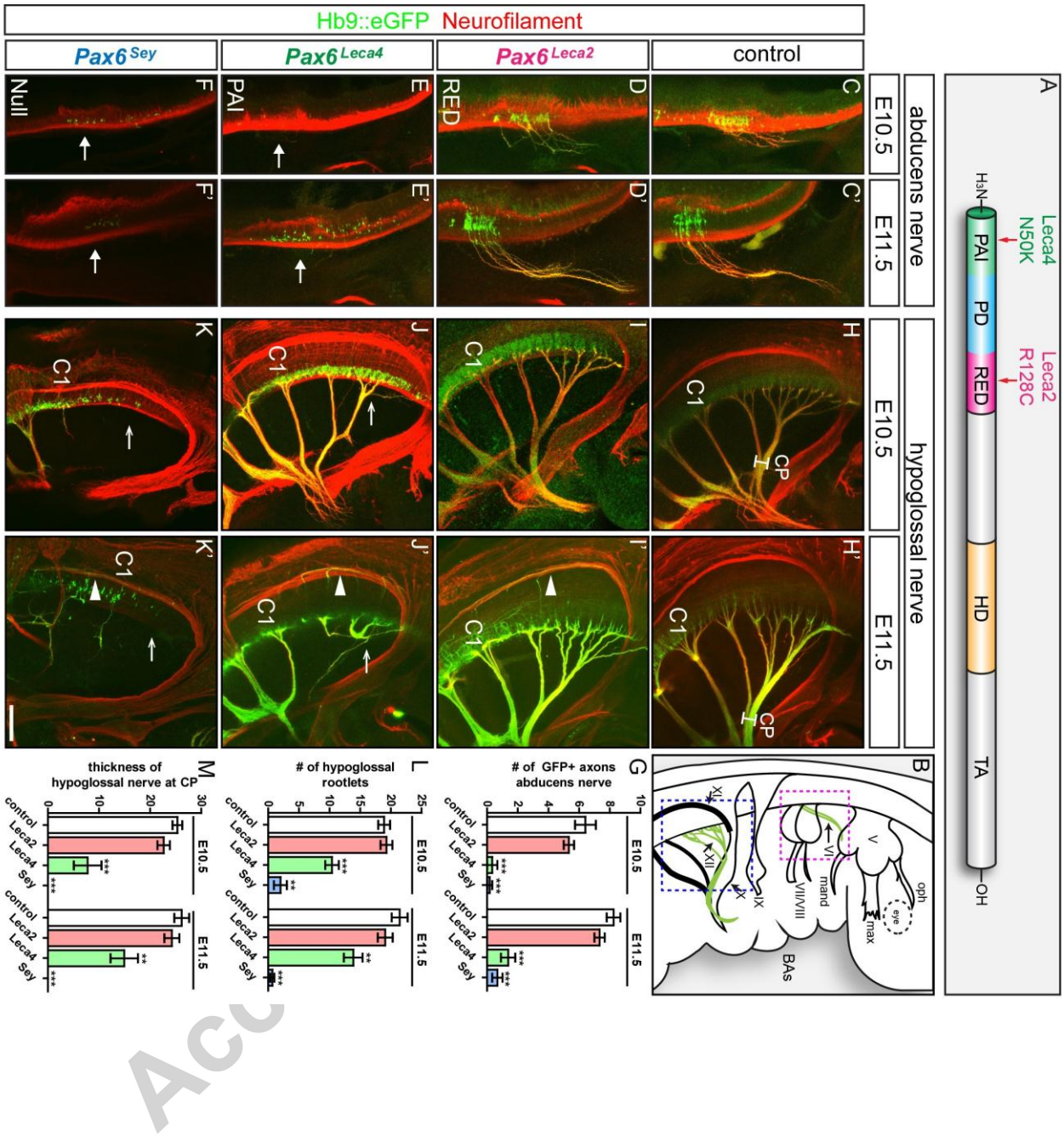
A
Leca4 N50K
Leca2 R128C
H3N
PAI
PD
RED
HD
TA
OH
B
oph
eye
max
V
Vi
mand
VII/VIII
IX
X
XI
XII
BAs
Hb9::eGFP Neurofilament
control
Pax6 Leca2
Pax6 Leca4
Pax6 Sey
abducens nerve
hypoglossal nerve
E10.5
E11.5
C
C'
D
D'
E
E'
F
F'
RED
PAI
Null
H
H'
I
I'
J
J'
K
K'
C1
CP
G
# of GFP+ axons abducens nerve
L
# of hypoglossal rootlets
M
thickness of hypoglossal nerve at CP
control
Leca2
Leca4
Sey

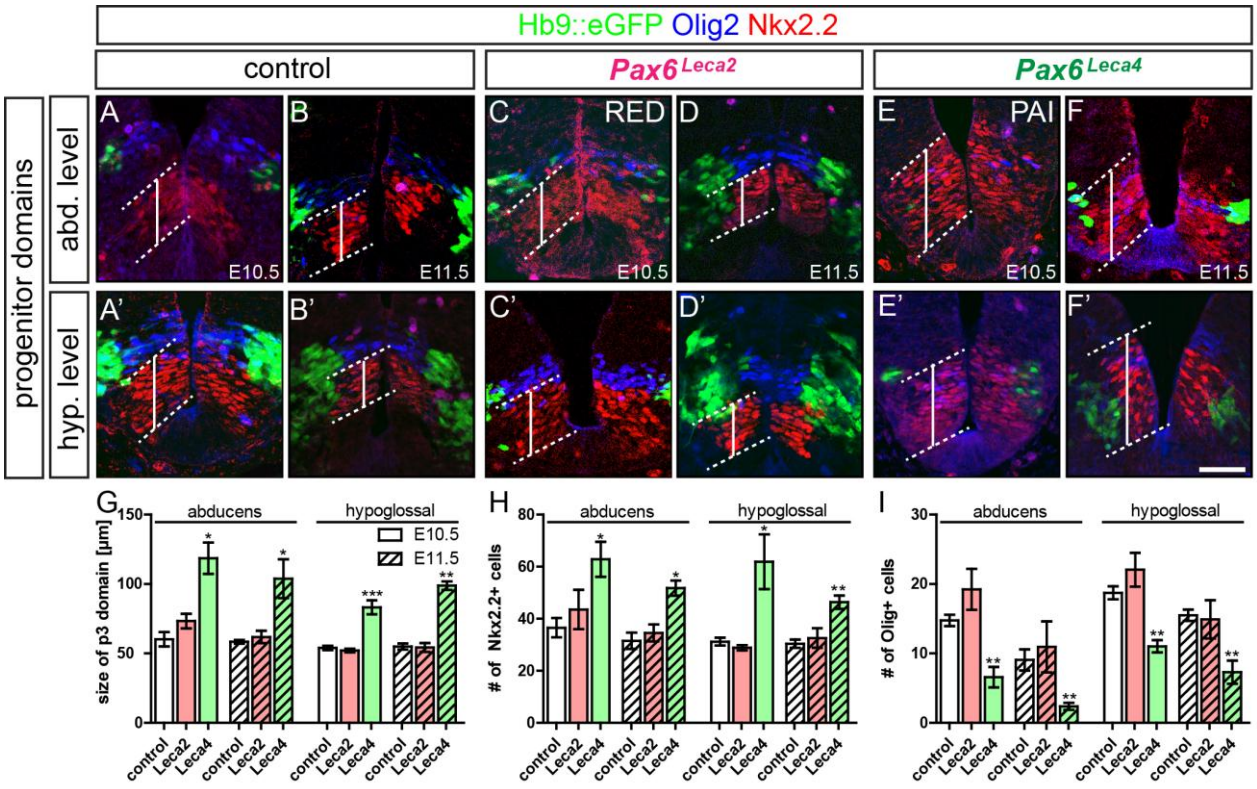

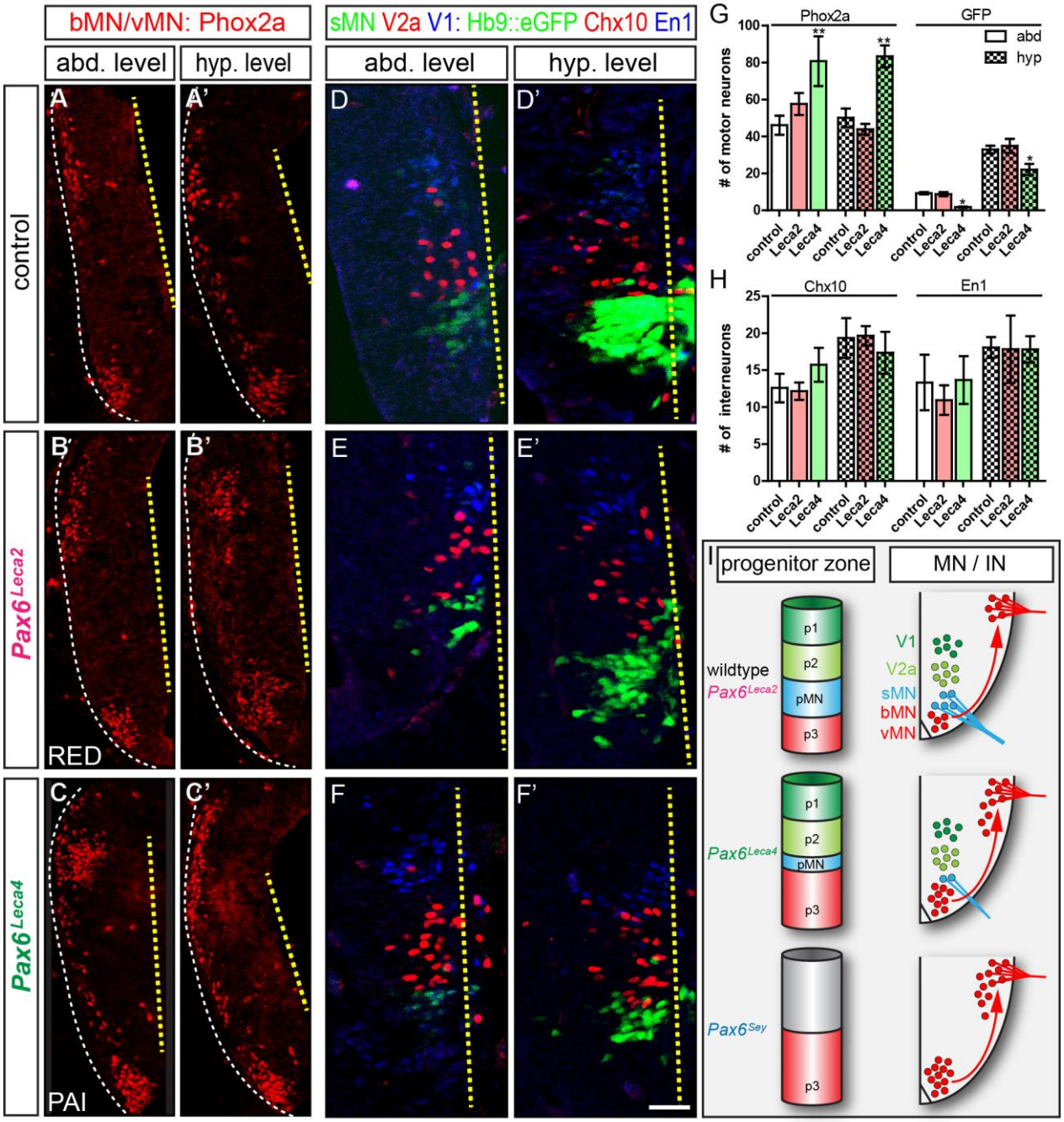
bMN/vMN: Phox2a
sMN V2a V1: Hb9::eGFP Chx10 En1
abd. level
hyp. level
abd. level
hyp. level
control
Pax6Leca2
Pax6Leca4
RED
PAI
A
A'
B
B'
C
C'
D
D'
E
E'
F
F'
G
Phox2a
GFP
abd
hyp
# of motor neurons
control
Leca2
Leca4
H
Chx10
En1
# of interneurons
I
progenitor zone
MN / IN
wildtype
Pax6Leca2
Pax6Leca4
Pax6Sey
p1
p2
pMN
p3
V1
V2a
sMN
bMN
vMN

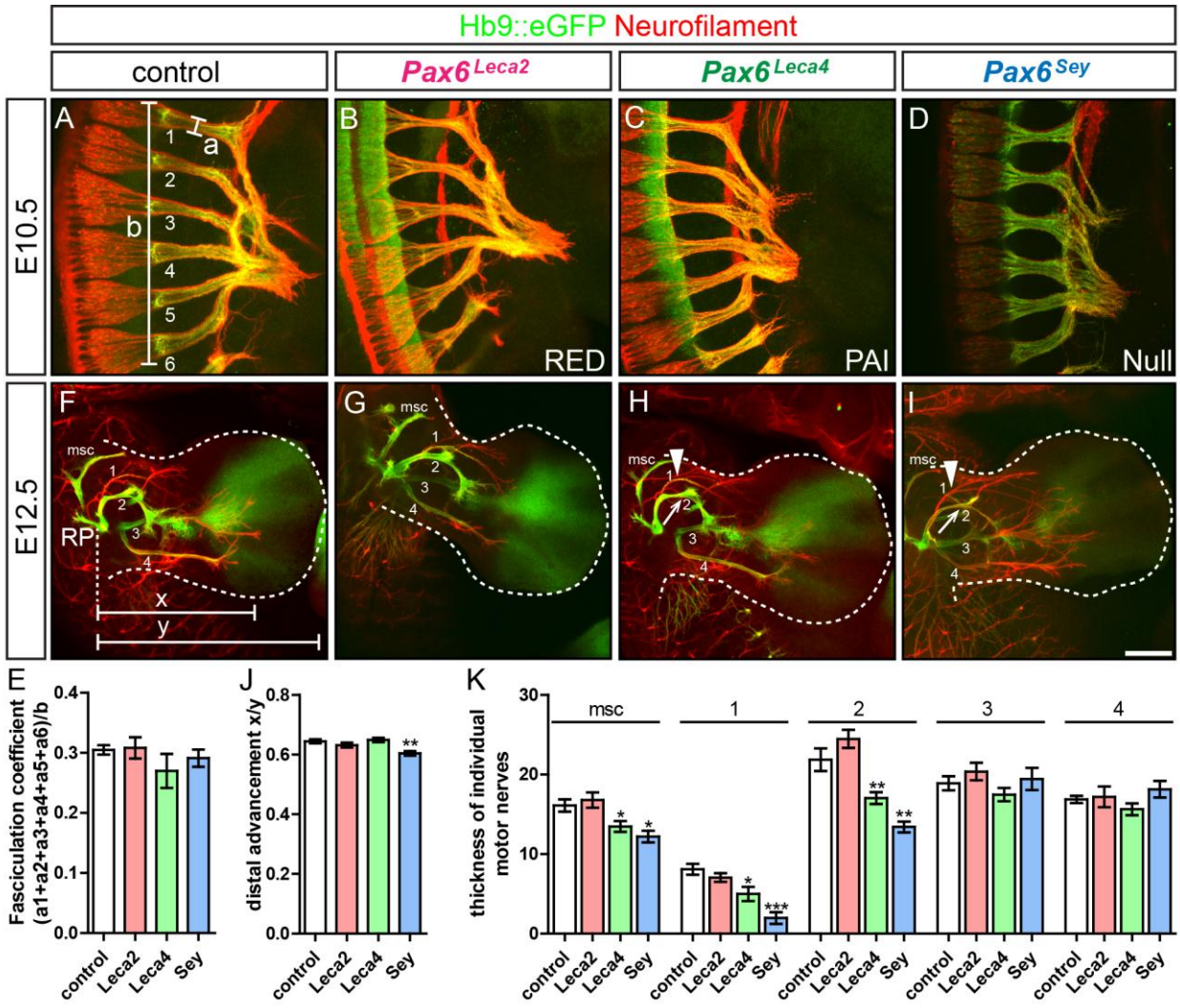
Hb9::eGFP Neurofilament
control
Pax6 Leca2
Pax6 Leca4
Pax6 Sey
E10.5
E12.5
A
B
C
D
F
G
H
I
RED
PAI
Null
msc
RP
a
b
x
y
E
J
K
Fasciculation coefficient (a1+a2+a3+a4+a5+a6)/b
distal advancement x/y
thickness of individual motor nerves
control
Leca2
Leca4
Sey

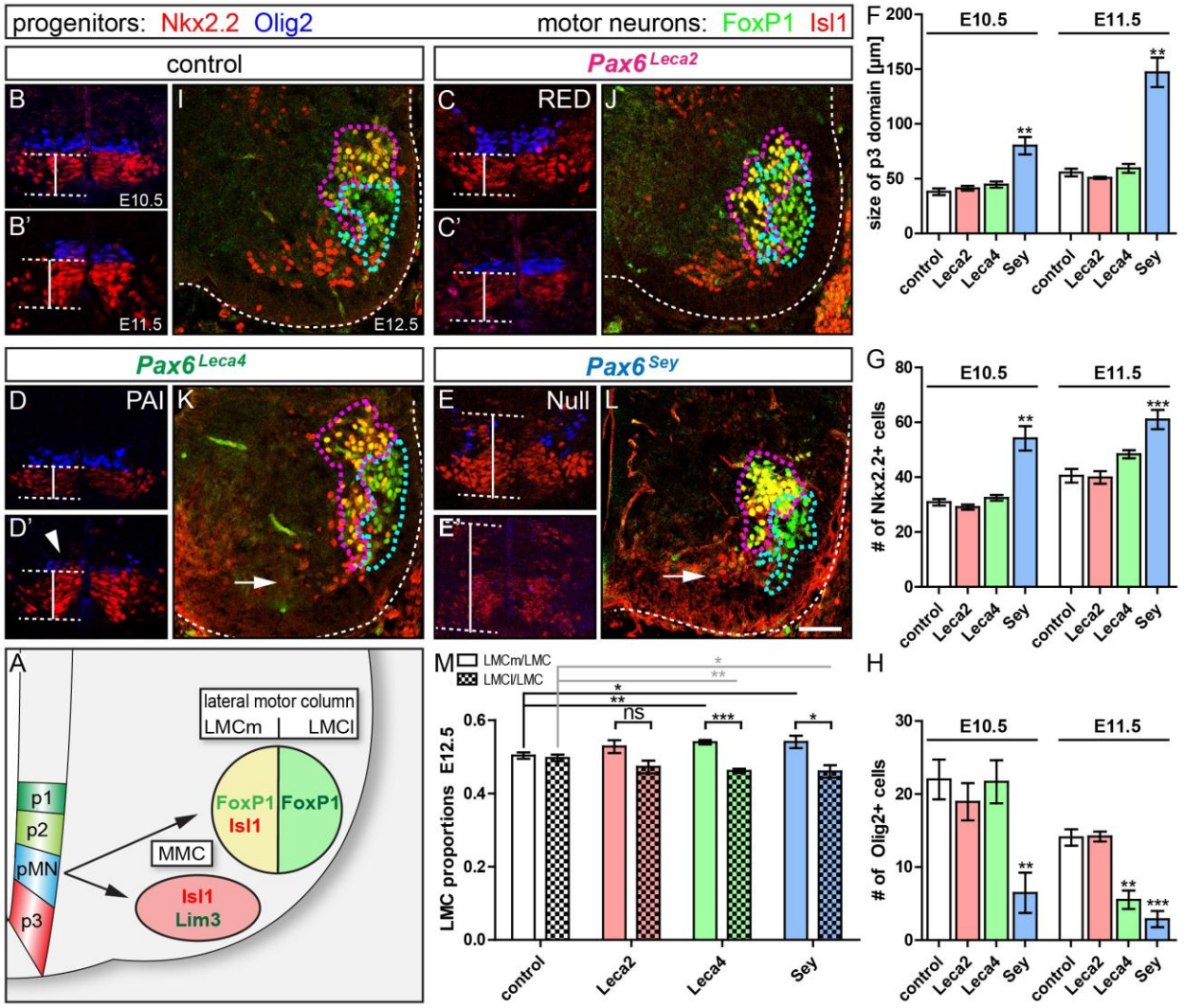
progenitors: Nkx2.2 Olig2
motor neurons: FoxP1 Isl1
control
Pax6 Leca2
Pax6 Leca4
Pax6 Sey
RED
PAI
Null
E10.5
E11.5
E12.5
lateral motor column
LMCm
LMCl
p1
p2
pMN
p3
FoxP1
Isl1
MMC
Lim3
LMCm/LMC
LMCl/LMC
LMC proportions E12.5
size of p3 domain [µm]
# of Nkx2.2+ cells
# of Olig2+ cells
control
Leca2
Leca4
Sey

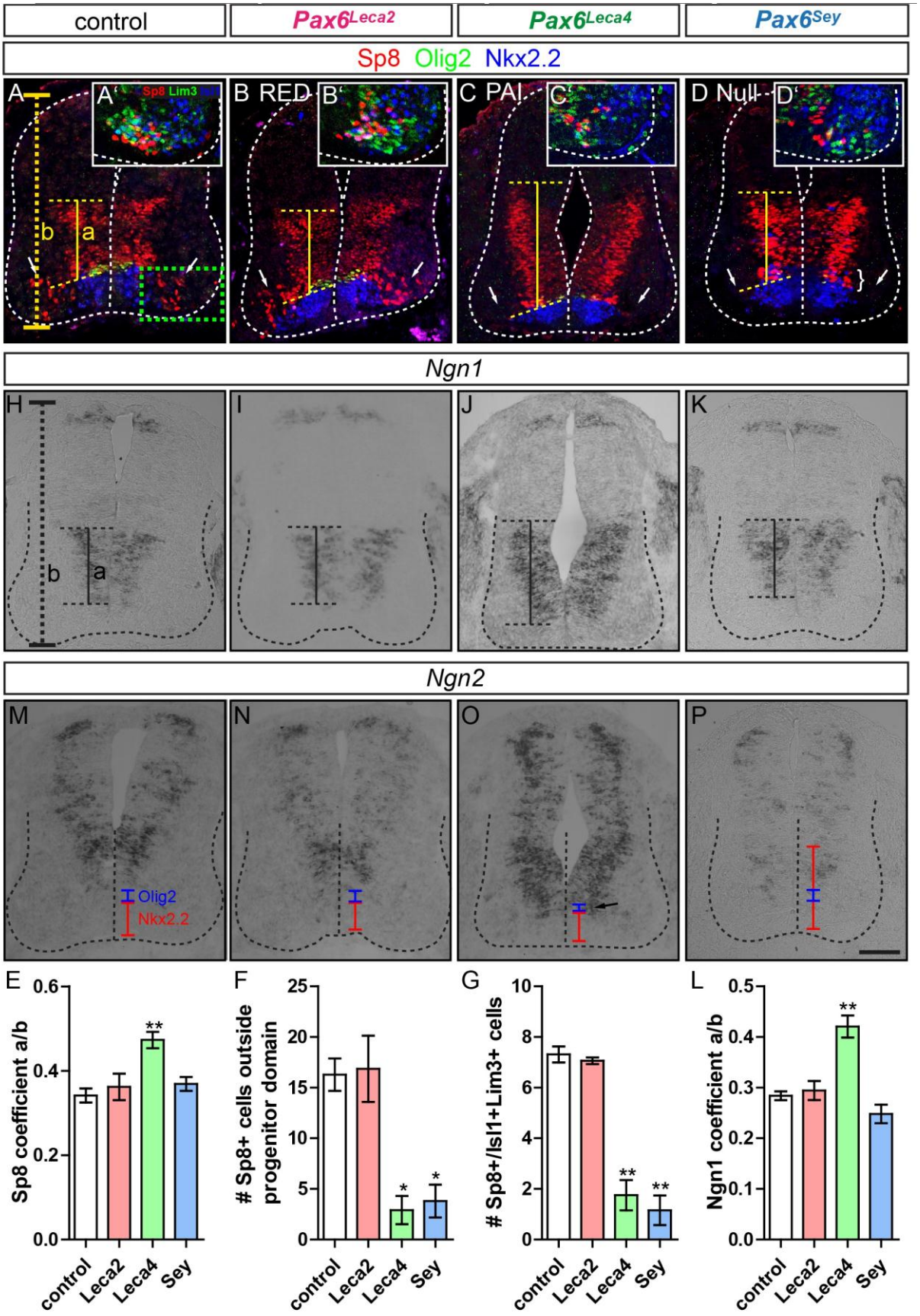
control
Pax6Leca2
Pax6Leca4
Pax6Sey
Sp8 Olig2 Nkx2.2
A
A'
Sp8 Lim3
B RED
B'
C PAI
C'
D Null
D'
b
a
Ngn1
H
I
J
K
Ngn2
M
N
O
P
Olig2
Nkx2.2
E
Sp8 coefficient a/b
F
Sp8+ cells outside progenitor domain
G
Sp8+/Isl1+Lim3+ cells
L
Ngn1 coefficient a/b
control
Leca2
Leca4
Sey

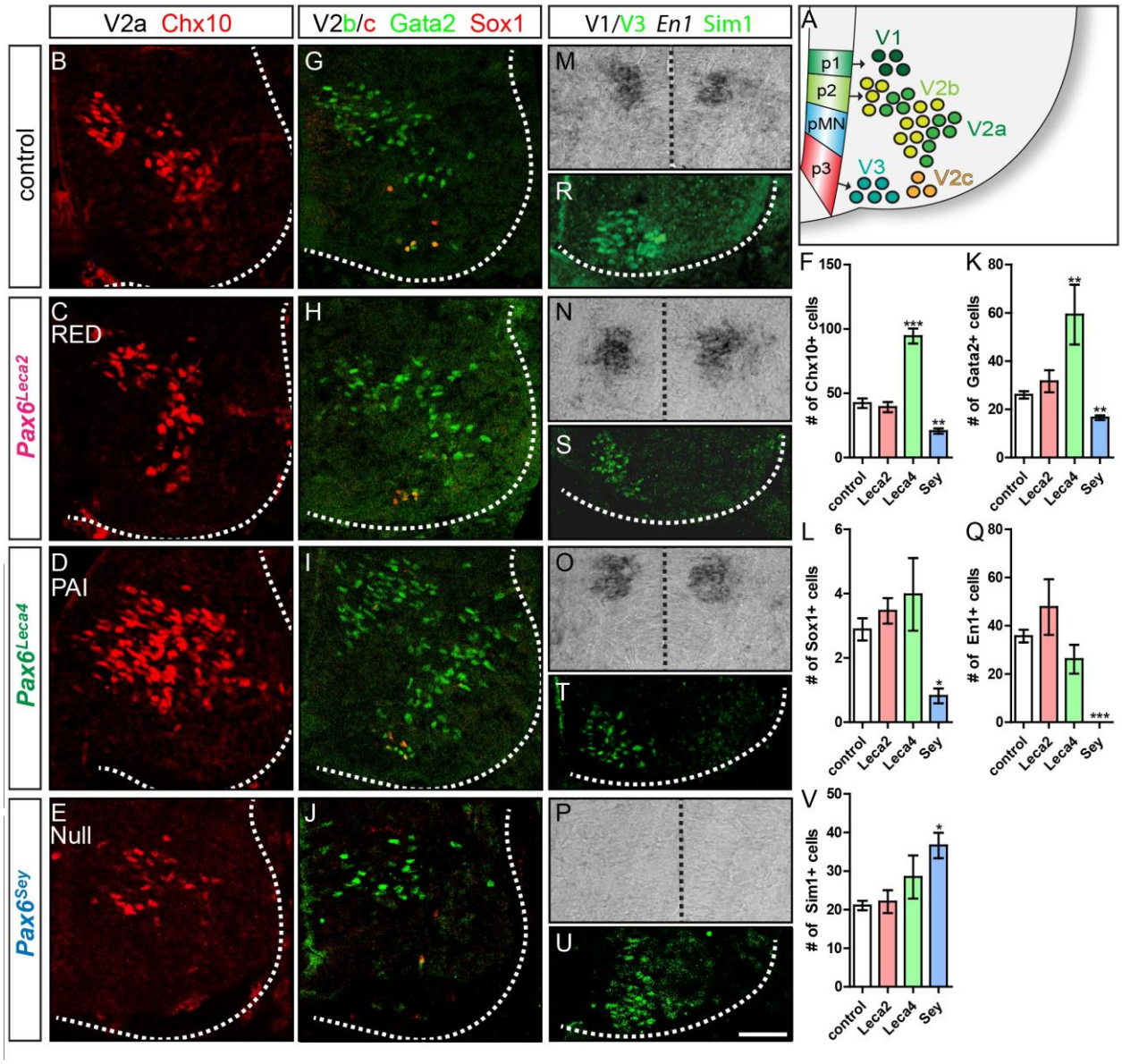
V2a Chx10
V2b/c Gata2 Sox1
V1/V3 En1 Sim1
control
Pax6Leca2
Pax6Leca4
Pax6Sey
B
G
M
R
C
RED
H
N
S
D
PAI
I
O
T
E
Null
J
P
U
A
V1
V2b
V2a
V2c
V3
p1
p2
pMN
p3
F
# of Chx10+ cells
K
# of Gata2+ cells
L
# of Sox1+ cells
Q
# of En1+ cells
V
# of Sim1+ cells
control
Leca2
Leca4
Sey

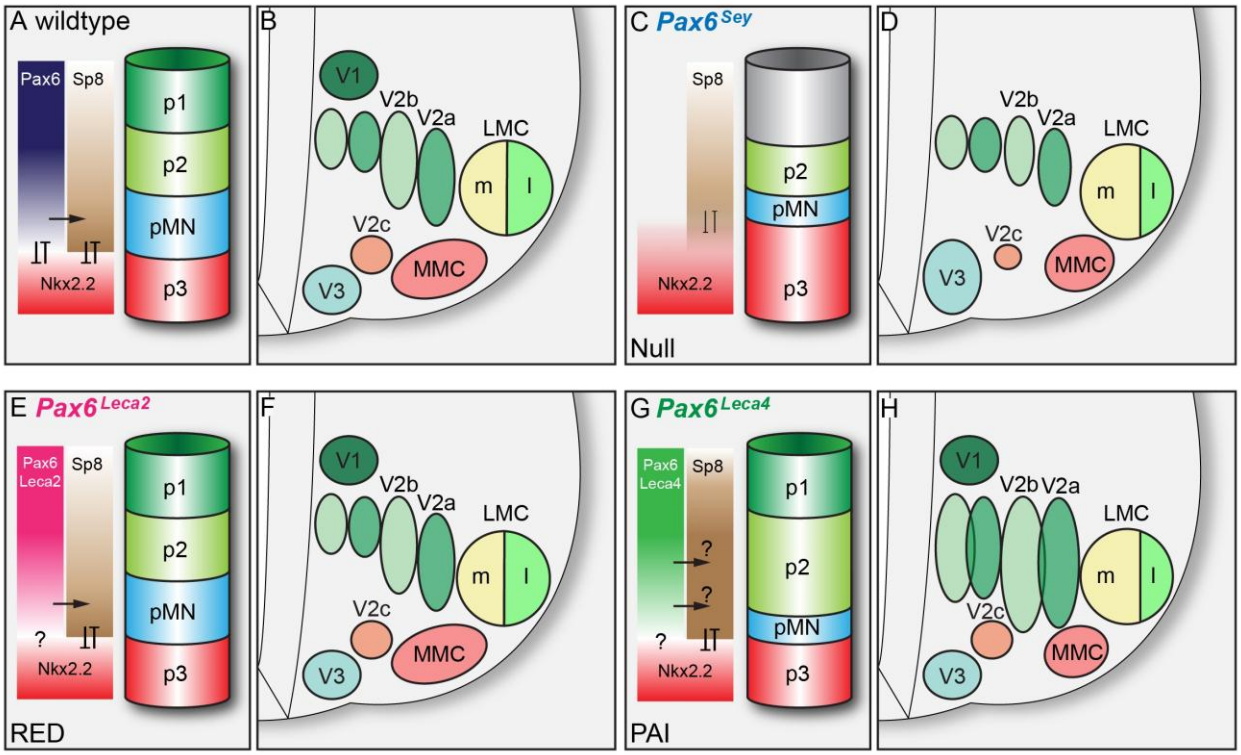

Highlights

The PAI sub-domain facilitates cranial p3-pMN boundary formation and sMN generation

Selective mutation of PD sub-domains does not impair cranial interneuron generation

The brachial p3-pMN boundary is not affected by selective mutation of PD sub-domains

The PAI sub-domain facilitates pMN-p2 boundary formation at brachial levels

Pax6 is involved in dorso-ventral and rostro-caudal neural tube patterning